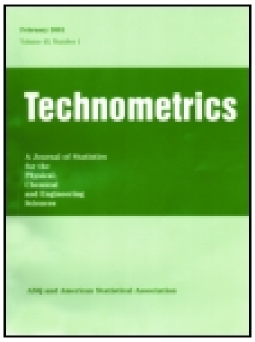

Technometrics

ISSN: 0040-1706 (Print) 1537-2723 (Online) Journal homepage: http://amstat.tandfonline.com/loi/utch20

Nonparametric finite mixture of Gaussian graphical models

Kevin H. Lee & Lingzhou Xue

To cite this article: Kevin H. Lee & Lingzhou Xue (2017): Nonparametric finite mixture of Gaussian graphical models, Technometrics, DOI: 10.1080/00401706.2017.1408497

To link to this article: https://doi.org/10.1080/00401706.2017.1408497

Accepted author version posted online: 30 Nov 2017.

Nonparametric finite mixture of Gaussian graphical models

Kevin H. Lee and Lingzhou Xue

Western Michigan University and Pennsylvania State University

Abstract

Graphical model has been widely used to investigate the complex dependence structure of high-dimensional data, and it is common to assume that observed data follow a homogeneous graphical model. However, observations usually come from different resources and have heterogeneous hidden commonality in real-world applications. Thus, it is of great importance to estimate heterogeneous dependencies and discover subpopulation with certain commonality across the whole population. In this work, we introduce a novel regularized estimation scheme for learning nonparametric finite mixture of Gaussian graphical models, which extends the methodology and applicability of Gaussian graphical models and mixture models. We propose a unified penalized likelihood approach to effectively estimate nonparametric functional parameters and heterogeneous graphical parameters. We further design an efficient generalized effective EM algorithm to address three significant challenges: high-dimensionality, non-convexity, and label switching. Theoretically, we study both the algorithmic convergence of our proposed algorithm and the asymptotic properties of our proposed estimators. Numerically, we demonstrate the performance of our method in simulation studies and a real application to estimate human brain functional connectivity from ADHD imaging data, where two heterogeneous conditional dependencies are explained through profiling demographic variables and supported by existing scientific findings.

Keywords. Gaussian graphical model, Nonparametric finite mixture, Non-convex optimization, Label switching, Brain imaging, Attention deficit hyperactivity disorder (ADHD).

1 Introduction

Graphical model has been widely used to investigate the complex dependence structure of high-dimensional data, and it has successful applications in various research fields. For example, in bioinformatics, graphical model is used in exploring the patterns of association in gene expression data (Dobra et al. 2004, Schäfer & Strimmer 2005), binary genomic data (Wang et al. 2011, Xue et al. 2012), cell signaling data (Voorman et al. 2014), among others. Due to advances in functional magnetic resonance imaging (fMRI), investigating brain function connectivity becomes increasingly important (Ryali et al. 2012). Gaussian graphical model has been extensively used in estimating the functional connectivity in brain imaging (Ng et al. 2013, Varoquaux et al. 2010). The central question here is to infer conditional dependencies or independencies from high-dimensional fMRI data. In the current literature, it is common to assume that high-dimensional data come from a homogeneous resource and follow a parametric or semiparametric graphical model, for instance, Gaussian graphical model and its variants (Meinshausen & Bühlmann 2006, Yuan & Lin 2007, Friedman et al. 2008, Peng et al. 2009, Witten et al. 2011, Cai et al. 2011, Liu et al. 2012, Xue & Zou 2012, Chandrasekaran et al. 2012, Ma et al. 2013, Danaher et al. 2014).

However, it is very common in real-world applications that observed data come from different resources and may have heterogeneous dependencies across the whole population. For instance, genetic variations data and gene expression data of the international HapMap project (Consortium 2010) consist of four representative populations in the world. Our research is motivated by exploring the heterogeneous dependencies of human brain fMRI data to study the Attention Deficit Hyperactivity Disorder (ADHD). The famous ADHD-200 Global Competition data (Biswal et al. 2010) aggregated across 8 independent imaging sites. Thus, it is very important to estimate heterogeneous dependencies and discover subpopulation with certain commonality. In the current literature, there are two different arguments about whether the gender affects the ADHD. On the one hand, some studies show that there is a gender difference in ADHD (Sauver et al. 2004). On the other hand, other studies argue that the ADHD is not systematically different between boys and girls (Bauermeister et al. 2007). It is likely that there may exist two different subpopulations with hidden commonality among the whole population, corresponding to two existing arguments respectively. Section 6 confirms this conjecture. More specifically, we show that both arguments may be explained through investigating heterogeneous brain functional connectivity using our proposed method.

In this work, we introduce a novel regularized estimation scheme for learning nonparametric finite mixture of Gaussian graphical models, which explores the heterogeneous dependencies of high-dimensional data. Denote by $\mathcal{G}^z(\mathbf{x}) = (\mathcal{V}, \mathcal{E}^z)$ the graphical model of random vector $\mathbf{x} \in \mathbb{R}^p$ with a univariate covariate $Z = z$, vertex set $\mathcal{V} = \{1, \ldots, p\}$ and edge set $\mathcal{E}^z$, where edge set $\mathcal{E}^z$ may depend on z. Let K be number of mixtures. Let $\mathcal{G}_k^z(\mathbf{x}) = (\mathcal{V}, \mathcal{E}_k^z)$ represent the Gaussian graphical model in the k-th subpopulation. Define $\mathcal{C}$ as the latent class variable satisfying that $P(\mathcal{C} = k|Z = z) = \pi_k(z)$, where $\pi_k(z)$ is a nonparametric mixing proportion function. Throughout this paper, we consider the following nonparametric finite mixture of Gaussian graphical models given some covariate $Z = z$:

$$\mathcal{G}^z(\mathbf{x}) = \pi_1(z)\mathcal{G}_1^z(\mathbf{x}) + \pi_2(z)\mathcal{G}_2^z(\mathbf{x}) + \cdots + \pi_K(z)\mathcal{G}_K^z(\mathbf{x}), \tag{1}$$

where $\pi_k(\cdot)$'s are nonparametric mixing proportion functions, and $\pi_1(z) + \ldots + \pi_K(z) = 1$ for any $z \in \mathbb{R}$. Mixture models are powerful to effectively identify subpopulations with hidden commonality within the whole population (Lindsay 1995, McLachlan & Peel 2004). The nonparametric Bayesian estimation of mixtures of Gaussian graphical models have been developed, for instance, Rodríguez et al. (2011). Under the fixed dimensional setting, Mallapragada et al. (2010) and Huang et al. (2013) studied the nonparametric finite mixture model for clustering and regression analysis respectively. Mixture models were extensively studied in the classical low-dimensional scenarios, but receive less attention in high-dimensional statistical learning. Recently, Städler et al. (2010) studied ℓ_1 penalization for mixtures of high-dimensional regression models, and Ruan et al. (2011) studied mixtures of Gaussian graphical models. However, it is a significant challenging to learn nonparametric finite mixture of Gaussian graphical models (1) in the presence of high-dimensionality, non-convexity and label switching. In Section 2, we propose a unified penalized likelihood approach to effectively estimate both nonparametric functional parameters and heterogeneous graphical parameters. To estimate nonparametric functional parameters, we adopt the idea of kernel regression technique and employ a local likelihood approach. Section 3 designs an efficient generalized effective EM algorithm to address three aforementioned challenges simultaneously. Furthermore, we propose an effective criterion to choose the number of mixtures, tuning parameter and bandwidth. We study the algorithmic convergence of our EM algorithm and the asymptotic result of our estimates in Section 4. Simulation studies and the real application to time-varying brain functional connectivity estimation are demonstrated in Sections 5 and 6 respectively. In Section 6, we discover two heterogeneous dependencies in the ADHD brain functional connectivity, which are explained through profiling demographic variables and supported by existing scientific findings. Our results provide helpful insights to study two different ADHD subpopulations with hidden commonality.

The contributions of our work can be summarized as follows. Methodologically, the proposed regularized estimation of nonparametric finite mixture of graphical models greatly extends the methodology and applicability of time-varying graphical models (Ahmed & Xing 2009, Kolar et al. 2010, Zhou et al. 2010) and finite mixture of graphical models (Ruan et al. 2011) for the analysis of high-dimensional data. Computationally, we design a novel efficient generalized effective EM algorithm to effectively estimate the nonparametric finite mixture and functional parameters, which addresses high-dimensionality, non-convexity and label switching simultaneously. Theoretically, we provide a new paradigm to not only prove the local convergence of the proposed generalized effective EM algorithm but also study the asymptotic properties of the local solution to the nonparametric finite mixture for high-dimensional data.

2 Methodology

Given some univariate covariate $Z = z$, nonparametric finite mixture (1) entails that $\mathbf{X} = \mathbf{x}$ follows a nonparametric finite mixture of multivariate Gaussian distributions:

$$\mathbf{X} = \mathbf{x} \mid Z = z \sim_d \sum_{k=1}^{K} \pi_k(z) N_p(\boldsymbol{\mu}_k(z), \boldsymbol{\Sigma}_k(z)), \tag{2}$$

where $\mathcal{G}_k^z(\mathbf{x})$ corresponds to a multivariate normal distribution $N_p(\boldsymbol{\mu}_k(z), \boldsymbol{\Sigma}_k(z))$ for $k = 1, \ldots, K$. Compared to the parametric finite mixture, the nonparametric mixing probabilities $\pi_k(z)$'s achieve the appealing robustness to model misspecification. We discuss the selection of the number of mixtures K in Section 3.2. We may also follow Rodríguez et al. (2011) to consider a nonparametric Bayesian approach to study the Dirichlet process mixtures of Gaussian graphical models when the underlying clusters are unknown. For space consideration, we do not pursue this alternative approach in this paper.

Let $\boldsymbol{\Theta}_k(z) = (\theta_{kij}(z))_{p\times p}$ be the precision matrix in the k-th mixture. Then, $\theta_{kij}(z)$'s specify the graphical model $\mathcal{G}_k^z(\mathbf{x})$ in the k-th mixture (Dempster 1972). Specifically, given $Z = z$, zeroes in $\theta_{kij}(z)$'s are equivalent to conditional independencies of $\mathbf{X}$ in the k-th mixture. Thus, zeroes in $\theta_{kij}(z)$'s can be translated to a meaningful graphical model:

$$\theta_{kij}(z) \neq 0 \iff X_i \not\perp\!\!\!\perp X_j \mid \mathbf{X} \setminus \{X_i, X_j\}, \mathcal{C} = k, Z = z \iff \{i, j\} \in \mathcal{E}_k^z.$$

For ease of presentation, we start with the known a priori number of mixtures K, and we present an effective information criterion to select K in Section 3.2.

Given the independent data $\{(\mathbf{x}_n, z_n), n = 1, \ldots, N\}$, our goal is to estimate nonparametric functions $\pi_k(\cdot)$'s and functional parameters $\boldsymbol{\mu}_k(\cdot)$'s and $\boldsymbol{\Theta}_k(\cdot)$'s. The global average log-likelihood function for the observed data is given by

$$\ell_N = \frac{1}{N}\sum_{n=1}^{N}\log\left[\sum_{k=1}^{K}\pi_k(z_n)\phi(\mathbf{x}_n|\boldsymbol{\mu}_k(z_n),\boldsymbol{\Theta}_k(z_n))\right].$$

where $\phi(\cdot|\boldsymbol{\mu},\boldsymbol{\Theta})$ is the density of a multivariate Gaussian distribution $N_p(\boldsymbol{\mu},\boldsymbol{\Theta}^{-1})$.

Next, we employ the local likelihood approach (Brillinger 1977, Tibshirani & Hastie 1987) to estimate $\pi_k(z)$'s, $\boldsymbol{\mu}_k(z)$'s, and $\boldsymbol{\Theta}_k(z)$'s for any $z \in \mathbb{R}$, given smoothness assumptions of such functional parameters. The local likelihood was first mentioned by Brillinger (1977) as a method of smoothing, and it was formally introduced and studied in details by Tibshirani & Hastie (1987). The local likelihood method received considerable attention in the nonparametric regression modeling and nonparametric function estimation (Loader 1996, 2006). Now, we follow Tibshirani & Hastie (1987) to define the localized version of the average log-likelihood function as

$$\ell_z \;=\; \frac{1}{N}\sum_{n=1}^{N}\log\left[\sum_{k=1}^{K}\pi_k^z\phi(\mathbf{x}_n|\boldsymbol{\mu}_k^z,\boldsymbol{\Theta}_k^z)\right]K_h(z_n-z),$$

where $K_h(\cdot)=h^{-1}K(\cdot/h)$ is a symmetric kernel function with bandwidth h. Given the local log-likelihood ℓ_z, we then maximize the ℓ_1-penalized local log-likelihood to estimate local constants π_k^z's, vectors $\boldsymbol{\mu}_k^z$'s, and matrices $\boldsymbol{\Theta}_k^z$'s as follows:

$$\max_{\{(\pi_k^z,\boldsymbol{\mu}_k^z,\boldsymbol{\Theta}_k^z)\}_{k=1,\ldots,K}}\mathcal{L}_z \quad := \quad \max_{\{(\pi_k^z,\boldsymbol{\mu}_k^z,\boldsymbol{\Theta}_k^z)\}_{k=1,\ldots,K}}\ell_z-\lambda\sum_{k=1}^{K}\|\boldsymbol{\Theta}_k^z\|_1, \tag{3}$$

where $\|\cdot\|_1$ is the entrywise matrix ℓ_1 norm. Instead of ℓ_1 penalization, we may also consider the folded concave penalized estimation to encourage sparsity in $\boldsymbol{\Theta}_k^z$'s (Fan et al. 2009, 2014). For space consideration, we only focus on the ℓ_1 penalization.

Remark 1. When $K=1$, nonparametric finite mixture of graphical models (1) reduces to covariate-dependent graphical model. When the covariate Z represents the varying time, $\mathcal{G}^z(\mathbf{x})$ becomes time-varying graphical model (Ahmed & Xing 2009, Kolar et al. 2010, Zhou et al. 2010), which is solved by using the penalized likelihood approach:

$$\hat{\boldsymbol{\Theta}}^z = \arg\max_{\boldsymbol{\Theta}^z}\ \frac{1}{N}\sum_{n=1}^{N}\log\left[\phi(\mathbf{x}_n|\boldsymbol{\mu}^z,\boldsymbol{\Theta}^z)\right]K_h(z_n-z)-\lambda\|\boldsymbol{\Theta}^z\|_1.$$

Remark 2. When $\mathcal{E}_k$ does not depend on covariate z, nonparametric finite mixture (1) reduces to semiparametric finite mixture of graphical models. Let $\mathcal{G}_k(\mathbf{x})=(\mathcal{V},\mathcal{E}_k)$ be the k-th mixture. The semiparametric finite mixture becomes $\mathcal{G}^z(\mathbf{x})=\pi_1(z)\mathcal{G}_1(\mathbf{x})+\cdots+\pi_K(z)\mathcal{G}_K(\mathbf{x})$, where

$\pi_1(z) + \ldots + \pi_K(z) = 1$ for any $z \in \mathbb{R}$. Conditioning on $Z = z$, $\mathbf{x}$ follows a semiparametric finite mixture $\sum_{k=1}^K \pi_k(z) N_p(\boldsymbol{\mu}_k, \boldsymbol{\Sigma}_k)$. Now we introduce local constants π_k^z's to approximate $\pi_k(z)$'s. Next, we may solve local estimates and global estimates of $\boldsymbol{\Theta}_k$'s. Firstly, we solve local constants $\tilde{\pi}_k^z$'s from

$$\max_{\{(\pi_k^z, \boldsymbol{\Theta}_k)\}_{k=1,\ldots,K}} \frac{1}{N} \sum_{n=1}^N \log \left[\sum_{k=1}^K \pi_k^z \phi(\mathbf{x}_n | \boldsymbol{\mu}_k, \boldsymbol{\Theta}_k) \right] K_h(z_n - z) - \lambda \sum_{k=1}^K \|\boldsymbol{\Theta}_k\|_1.$$

After obtaining local estimates $\tilde{\pi}_k(z_n)$'s for $n = 1, \ldots, N$, we solve global estimates via

$$\max_{\{\boldsymbol{\Theta}_k\}_{k=1,\ldots,K}} \frac{1}{N} \sum_{n=1}^N \log \left[\sum_{k=1}^K \tilde{\pi}_k(z_n) \phi(\mathbf{x}_n | \boldsymbol{\mu}_k, \boldsymbol{\Theta}_k) \right] - \lambda \sum_{k=1}^K \|\boldsymbol{\Theta}_k\|_1.$$

Remark 3. When there is no covariate, nonparametric finite mixture (1) further reduces to finite mixture of Gaussian graphical models (Ruan et al. 2011), i.e.

$$\mathcal{G}(\mathbf{x}) = \pi_1 \mathcal{G}_1(\mathbf{x}) + \pi_2 \mathcal{G}_2(\mathbf{x}) + \cdots + \pi_K \mathcal{G}_K(\mathbf{x}),$$

that is, $\mathbf{x} \sim_d \sum_{k=1}^K \pi_k N_p(\boldsymbol{\mu}_k, \boldsymbol{\Sigma}_k)$, where $\pi_1 + \ldots + \pi_K = 1$. This can be solved by

$$\max_{\{(\pi_k, \boldsymbol{\Theta}_k)\}_{k=1,\ldots,K}} \frac{1}{N} \sum_{n=1}^N \log \left[\sum_{k=1}^K \pi_k \phi(\mathbf{x}_n | \boldsymbol{\mu}_k, \boldsymbol{\Theta}_k) \right] - \lambda \sum_{k=1}^K \|\boldsymbol{\Theta}_k\|_1.$$

3 Computation

Expectation-Maximization (EM) algorithm provides a powerful tool to solve latent variable problems in mixture model. Wu (1983) established some general convergence properties, and Balakrishnan et al. (2014) recently studied the statistical guarantees on both population level and sample level. However, we need to address two significant challenges when solving the nonparametric finite mixture model (3): 1) non-convex optimization in high dimensions; 2) label switching issue at different grid points of covariate z. This section presents a generalized effective EM algorithm to address both challenges, which enjoys some appealing convergence properties as shown in Section 4.

3.1 Proposed EM algorithm

Following the spirit of EM algorithm, we view the collected data $(\mathbf{x}_n, z_n), n = 1, \dots, N$ to be incomplete, and then define random variables $\boldsymbol{\tau}_n = (\tau_{1n}, \dots, \tau_{Kn})'$ with

$$\tau_{kn} = \begin{cases} 1 & \text{if } (\mathbf{x}_n, z_n) \text{ is in the } k\text{-th mixture,} \\ 0 & \text{otherwise} \end{cases}$$

to identify the mixture of $(\mathbf{x}_n, z_n)$. Given the complete data $\{(\mathbf{x}_n, z_n, \boldsymbol{\tau}_n), n = 1, \dots, N\}$, the complete log-likelihood function is written as

$$\ell_N^{\text{cmp}} = \frac{1}{N} \sum_{n=1}^{N} \sum_{k=1}^{K} \tau_{kn} \left[\log \pi_k(z_n) + \log \phi(\mathbf{x}_n | \boldsymbol{\mu}_k(z_n), \boldsymbol{\Theta}_k(z_n)) \right].$$

Let $z \in \{u_1, \dots, u_G\}$, the set of grid points. We employ kernel regression techniques to estimate $\pi_k(z_n)$, $\boldsymbol{\mu}_k(z_n)$, and $\boldsymbol{\Theta}_k(z_n)$. Define a local complete log-likelihood as

$$\ell_z^{\text{cmp}} = \frac{1}{N} \sum_{n=1}^{N} \sum_{k=1}^{K} \tau_{kn} \left[\log \pi_k^z + \log \phi(\mathbf{x}_n | \boldsymbol{\mu}_k^z, \boldsymbol{\Theta}_k^z) \right] K_h(z_n - z).$$

Next, we define the ℓ_1-penalized local log-likelihood function for the complete data as

$$\mathcal{L}_z^{\text{cmp}} \ = \ \ell_z^{\text{cmp}} - \lambda \sum_{k=1}^{K} \|\boldsymbol{\Theta}_k^z\|_1.$$

Notice that there are potential label switching issues at any two different grid points $z, z' \in \mathcal{U} = \{u_1, \dots, u_G\}$. To solve this issue, we propose the following generalized effective EM algorithm. Given the current estimates of parameters, E-step estimates all conditional expectations (4) at observed $\{z_1, \dots, z_N\}$. M-step uses the obtained common conditional expectations to update all estimates of parameters at each grid point in $\mathcal{U}$. Hence, we effectively prevent the label switching issue at different grid points. As shown in Figure 1, two solution paths from simulation studies in Section 5 demonstrate that two mixtures are consistently identified at different grid points.

In what follows, we present algorithm details. Since only $(\mathbf{x}_n, z_n)$'s are observed, we treat $\boldsymbol{\tau}_n$'s as missing data. In the $(t+1)$-th iteration, $t = 0, 1, 2, \dots$, E-step employs the t-th iterated solution $\pi_k^{(t)}(z_n)$, $\boldsymbol{\mu}_k^{(t)}(z_n)$ and $\boldsymbol{\Theta}_k^{(t)}(z_n)$ to compute the conditional expectation of τ_{kn} given the current estimates. By using Bayes' rule, we have

$$\gamma_{kn}^{(t+1)} = \frac{\pi_k^{(t)}(z_n) \phi(\mathbf{x}_n | \boldsymbol{\mu}_k^{(t)}(z_n), \boldsymbol{\Theta}_k^{(t)}(z_n))}{\sum_{l=1}^{K} \pi_l^{(t)}(z_n) \phi(\mathbf{x}_n | \boldsymbol{\mu}_l^{(t)}(z_n), \boldsymbol{\Theta}_l^{(t)}(z_n))}. \tag{4}$$

Figure 1: Solution path at six different grid points: 1st mixture (upper panel) and 2nd mixture (lower panel).

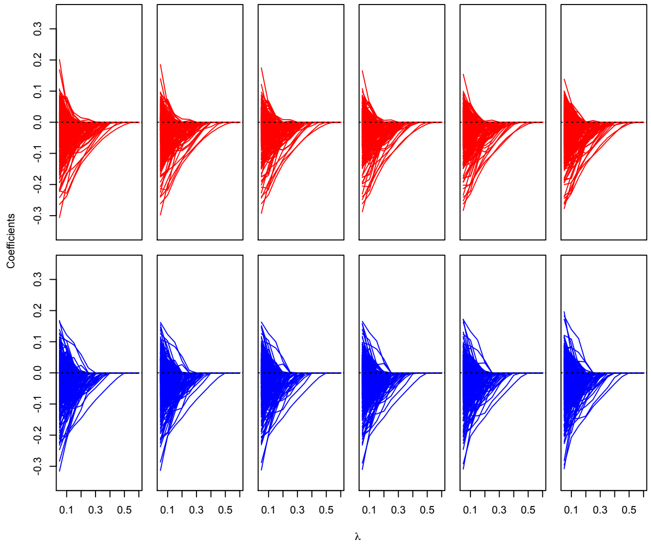

Next, M-step obtains the estimates of parameters from maximizing

$$\frac{1}{N}\sum_{n=1}^{N}\sum_{k=1}^{K}\gamma_{kn}^{(t+1)}\left[\log\pi_k^z+\log\phi(\mathbf{x}_n|\boldsymbol{\mu}_k^z,\boldsymbol{\Theta}_k^z)\right]K_h(z_n-z)-\lambda\sum_{k=1}^{K}\|\boldsymbol{\Theta}_k^z\|_1$$

subject to the constraint that $\sum_{k=1}^{K}\pi_k^z=1$. It is equivalent to maximizing

$$\frac{1}{N}\sum_{n=1}^{N}\sum_{k=1}^{K}\gamma_{kn}^{(t+1)}\log\pi_k^zK_h(z_n-z), \tag{5}$$

subject to $\sum_{k=1}^{K}\pi_k^z=1$, and for $k=1,\ldots,K$, maximizing

$$\frac{1}{N}\sum_{n=1}^{N}\gamma_{kn}^{(t+1)}\log\phi(\mathbf{x}_n|\boldsymbol{\mu}_k^z,\boldsymbol{\Theta}_k^z)K_h(z_n-z)-\lambda\|\boldsymbol{\Theta}_k^z\|_1, \tag{6}$$

respectively. To solve the subproblem (5), we introduce Lagrange multiplier α with the constraint $\sum_{k=1}^{K}\pi_k^z=1$. Then in the $(t+1)$-th cycle, for $z\in\{u_g,g=1,\ldots,G\}$ we update π_k^z by

$$\pi_k^{z(t+1)}=\sum_{n=1}^{N}\frac{\gamma_{kn}^{(t+1)}K_h(z_n-z)}{\sum_{n'=1}^{N}K_h(z_{n'}-z)}. \tag{7}$$

In order to solve the subproblem (6), we first simplify (6) as,

$$\frac{1}{N}\sum_{n=1}^{N}\gamma_{kn}^{(t+1)}\left[\frac{1}{2}\log|\boldsymbol{\Theta}_k^z|-\frac{1}{2}(\mathbf{x}_n-\boldsymbol{\mu}_k^z)'\boldsymbol{\Theta}_k^z(\mathbf{x}_n-\boldsymbol{\mu}_k^z)\right]K_h(z_n-z)-\lambda\|\boldsymbol{\Theta}_k^z\|_1.$$

Then, it is easy to obtain the closed-form update for $\boldsymbol{\mu}_k^z$, that is

$$\boldsymbol{\mu}_k^{z(t+1)} = \sum_{n=1}^{N} \frac{\gamma_{kn}^{(t+1)} K_h(z_n - z)\mathbf{x}_n}{\sum_{n'=1}^{N} \gamma_{kn'}^{(t+1)} K_h(z_{n'} - z)}. \tag{8}$$

Next, we employ the state-of-art optimization algorithm such as Friedman et al. (2008), Witten et al. (2011) and Goldfarb et al. (2013) and to solve $\boldsymbol{\Theta}_k^z$ from

$$\boldsymbol{\Theta}_k^{z(t+1)} = \arg\max_{\boldsymbol{\Theta}_k^z} \left\{ \log|\boldsymbol{\Theta}_k^z| - \mathrm{tr}(\boldsymbol{\Theta}_k^z \mathbf{A}_k^{z(t+1)}) - \lambda \|\boldsymbol{\Theta}_k^z\|_1 \right\}, \tag{9}$$

where $\mathbf{A}_k^{z(t+1)} = \sum_{n=1}^{N} \frac{\gamma_{kn}^{(t+1)} K_h(z_n - z)}{\sum_{n'=1}^{N} \gamma_{kn'}^{(t+1)} K_h(z_{n'} - z)} (\mathbf{x}_n - \boldsymbol{\mu}_k^{z(t+1)})(\mathbf{x}_n - \boldsymbol{\mu}_k^{z(t+1)})'$. Furthermore, we update $\pi_k^{(t+1)}(z_n)$, $\boldsymbol{\mu}_k^{(t+1)}(z_n)$, and $\boldsymbol{\Theta}_k^{(t+1)}(z_n)$, $n = 1, \dots, N$ by linear interpolating $\pi_k^{u_g(t+1)}$, $\boldsymbol{\mu}_k^{u_g(t+1)}$, and $\boldsymbol{\Theta}_k^{u_g(t+1)}$, $g = 1, \dots, G$ respectively. More details about (7), (8) and (9) are presented in the Appendix.

Now, we summarize the details of our proposed algorithm in Algorithm 1.

Algorithm 1 Proposed generalized effective EM algorithm

```
• Initialization of $\pi_k^{(0)}(z_n)$, $\boldsymbol{\mu}_k^{(0)}(z_n)$, and $\boldsymbol{\Theta}_k^{(0)}(z_n)$ for all $k$.
• Iteratively solve E-step and M-step with $t = 0, 1, \dots$ till convergence:
    – E-step: solve $\gamma_{kn}^{(t+1)}$ from (4) for all $k$ and $n$.
    – M-step: solve $\pi_k^{z(t+1)}$, $\boldsymbol{\mu}_k^{z(t+1)}$, $\boldsymbol{\Theta}_k^{z(t+1)}$ from (7)–(9) for all $k$ and $z$.
```

3.2 Selection of tuning parameters

We need to select three tuning parameters: number of mixtures K, penalization parameter λ, and bandwidth h. To determine them, we consider the information criterion approach. Bayesian Information Criterion (BIC) has the general form of $-2\mathcal{L} + \delta \times df$, where $\mathcal{L}$ is the maximum log-likelihood, $\delta = \log N$, and df is the degree of freedom to measure model complexity. To specify the degree of freedom in nonparametric finite mixture (2), we follow Fan et al. (2001) and Huang et al. (2013) to derive the degree of freedom. Denote by $\mathrm{df} = \tau_K h^{-1} |\mathcal{Z}| \left(K(0) - \frac{1}{2} \int K^2(t)\, dt \right)$ the degree of freedom of a univariate nonparametric function, where $\mathcal{Z}$ is the support of the covariate Z, and $\tau_K = \frac{K(0) - \frac{1}{2}\int K^2(t)\, dt}{\int \left(K(t) - \frac{1}{2} K * K(t) \right)^2 dt}$. Hence, for each pair of (K, λ, h), the BIC score is defined as

$$\mathrm{BIC}(K, \lambda, h) = -2\mathcal{L} + \log(N) \times df(K, \lambda, h),$$

where

$$df(K,\lambda,h) = \left[(K-1) + \frac{1}{G}\sum_{z\in\mathcal{U}}\left(Kp + \sum_{k=1}^{K}\sum_{i\leq j} I_{\{\hat{\Theta}^z_{ijk}\neq 0\}}\right)\right] \times \text{df}.$$

We first select K and λ by minimizing the BIC score, and then choose h by cross validation (CV). We choose K by minimizing the best available BIC score for each choice of K over different choices of λ and h. Namely,

$$\hat{K} = \arg\min_{(\lambda,h)} \text{BIC}(K,\lambda,h).$$

After fixing $K = \hat{K}$, we choose λ by minimizing the best available BIC score for each λ over different choices of h. Namely,

$$\hat{\lambda} = \arg\min_{h} \text{BIC}(\hat{K},\lambda,h).$$

Lastly, we use the log-likelihood to construct the CV loss, and choose h by CV.

4 Theoretical Properties

This section will first establish the algorithmic convergence of our proposed algorithm, and then prove the asymptotic properties of our proposed estimator.

4.1 Algorithmic convergence

Recall that $\mathcal{L}_z(\boldsymbol{\pi}^z, \boldsymbol{\mu}^z, \boldsymbol{\Theta}^z) = \ell_z(\boldsymbol{\pi}^z, \boldsymbol{\mu}^z, \boldsymbol{\Theta}^z) - \lambda\sum_{k=1}^{K}\|\boldsymbol{\Theta}^z_k\|_1$ is the objective function (3). Let $\left\{(\boldsymbol{\pi}^{z(t)}, \boldsymbol{\mu}^{z(t)}, \boldsymbol{\Theta}^{z(t)}) : t = 0,1,2,...\right\}$ be the sequence generated by Algorithm 1. Since the objective function is non-concave and non-differentiable, we study the local convergence of our proposed algorithm. To this end, we first define the *cluster point* in the sequence $\{(\boldsymbol{\pi}^{z(t)}, \boldsymbol{\mu}^{z(t)}, \boldsymbol{\Theta}^{z(t)}) : t = 0,1,2,\ldots\}$ generated by Algorithm 1, which is also known as "accumulation point" in mathematics or optimization theory.

Definition 1. For any given grid point z, $(\bar{\boldsymbol{\pi}}^z, \bar{\boldsymbol{\mu}}^z, \bar{\boldsymbol{\Theta}}^z)$ is called a *cluster point* in the sequence $\{(\boldsymbol{\pi}^{z(t)}, \boldsymbol{\mu}^{z(t)}, \boldsymbol{\Theta}^{z(t)}) : t = 0,1,2,\ldots\}$ if there exists a convergent subsequence $\{(\boldsymbol{\pi}^{z(t_j)}, \boldsymbol{\mu}^{z(t_j)}, \boldsymbol{\Theta}^{z(t_j)}) : j = 1,2,\ldots\}$ such that $(\boldsymbol{\pi}^{z(t_j)}, \boldsymbol{\mu}^{z(t_j)}, \boldsymbol{\Theta}^{z(t_j)}) \to (\bar{\boldsymbol{\pi}}^z, \bar{\boldsymbol{\mu}}^z, \bar{\boldsymbol{\Theta}}^z)$.

Next, we follow Tseng (2001) and Städler et al. (2010) to define the stationary point under the non-concave and non-differentiable maximization:

Definition 2. Let u be a function defined on some open set U. A point $s \in U$ is called a *stationary point* if the directional derivative $u'(s;d) = \lim_{\alpha\downarrow 0}\frac{u(s+\alpha d)-u(s)}{\alpha} \leq 0, \quad \forall d.$

We first show that Algorithm 1 preserves the nice ascent property as the classical EM algorithm with probability tending to 1.

Theorem 1. *Suppose $h \to 0$ and $Nh \to \infty$ as $N \to \infty$. For any given point z and $t = 0, 1, 2, ...$, with probability tending to 1, we always have*

$$\mathcal{L}_z(\boldsymbol{\pi}^{z(t+1)}, \boldsymbol{\mu}^{z(t+1)}, \boldsymbol{\Theta}^{z(t+1)}) \geq \mathcal{L}_z(\boldsymbol{\pi}^{z(t)}, \boldsymbol{\mu}^{z(t)}, \boldsymbol{\Theta}^{z(t)}),$$

and $\{\mathcal{L}_z(\boldsymbol{\pi}^{z(t)}, \boldsymbol{\mu}^{z(t)}, \boldsymbol{\Theta}^{z(t)}) : \ t = 0, 1, 2, \ldots\}$ increases monotonically to some $\bar{\mathcal{L}} < \infty$.

Given the ascent property in Theorem 1, we are ready to prove the local convergence result of our proposed EM algorithm in the following theorem. Theorem 2 extends the local convergence result of Städler et al. (2010) to the nonparametric finite mixture (1).

Theorem 2. *Under the same conditions of Theorem 1, with probability tending to 1, our proposed generalized effective EM algorithm (i.e. Algorithm 1) achieves the local convergence. More specifically, for any given z, every cluster point $(\bar{\boldsymbol{\pi}}^z, \bar{\boldsymbol{\mu}}^z, \bar{\boldsymbol{\Theta}}^z)$ in the sequence $\{(\boldsymbol{\pi}^{z(t)}, \boldsymbol{\mu}^{z(t)}, \boldsymbol{\Theta}^{z(t)}) : t = 0, 1, 2, \ldots\}$ is a stationary point of the objective function $\mathcal{L}_z(\boldsymbol{\pi}^z, \boldsymbol{\mu}^z, \boldsymbol{\Theta}^z)$ in (3) with probability tending to 1.*

Remark 4. When learning the nonparametric finite mixture of Gaussian graphical models, Theorems 1–2 prove that both the ascent property and the local convergence hold for Algorithm 1 with probability tending to 1. It is obvious that Theorems 1–2 can be easily extended to the semiparametric finite mixture $\mathcal{G}^z(\mathbf{x}) = \pi_1(z)\mathcal{G}_1(\mathbf{x}) + \cdots + \pi_K(z)\mathcal{G}_K(\mathbf{x})$ in Remark 2. When there is no covariate z, we may further extend Theorems 1–2 and obtain the exact ascent property that $\mathcal{L}(\boldsymbol{\pi}^{(t+1)}, \boldsymbol{\mu}^{(t+1)}, \boldsymbol{\Theta}^{(t+1)}) \geq \mathcal{L}(\boldsymbol{\pi}^{(t)}, \boldsymbol{\mu}^{(t)}, \boldsymbol{\Theta}^{(t)})$ and the exact local convergence for the finite mixture of Gaussian graphical models $\mathcal{G}(\mathbf{x}) = \pi_1\mathcal{G}_1(\mathbf{x}) + \cdots + \pi_K\mathcal{G}_K(\mathbf{x})$ proposed by Ruan et al. (2011) in Remark 3.

4.2 Asymptotic properties

Let $\boldsymbol{\omega}(z) = (\boldsymbol{\pi}(z), \boldsymbol{\mu}(z), \boldsymbol{\Theta}(z))$ be the true functional parameters in model (2). Define vec$(\cdot)$ as the vectorization of a matrix. We introduce some regularity conditions.

A. $\{(\mathbf{x}_n, z_n), n = 1, \ldots, N\}$ are independent and identically distributed as $(\mathbf{X}, Z)$. The support for Z, denoted by $\mathcal{Z}$, is compact subset of $\mathbb{R}^1$.

B. $\boldsymbol{\omega}(z)$ have continuous second derivatives, and $\pi_k(z) > 0$ for any $z \in \mathcal{Z}$.

C. The marginal density $f(z)$ of Z is twice continuously differentiable and positive.

D. The kernel function $K(\cdot)$ is symmetric, continuous, and has a closed and bounded support and satisfy following conditions:

$$\int K(u)\,du = 1, \quad \int uK(u)\,du = 0, \quad \int u^2 K(u)\,du < \infty,$$
$$\int K^2(u)\,du < \infty, \quad \int |K^3(u)|\,du < \infty.$$

E. There exists a function $M(\mathbf{x})$ with $\mathrm{E}[M(\mathbf{X})] < \infty$, such that for all $\mathbf{x}$ and all $\boldsymbol{\omega}^z$ in a neighborhood of $\boldsymbol{\omega}(z)$, $|\partial^3 \ell(\boldsymbol{\omega}(z), \mathbf{x})/\partial\omega_i \partial\omega_j \partial\omega_l| < M(\mathbf{x})$ holds.

F. $\mathrm{E}\left(\left|\frac{\partial \ell(\boldsymbol{\omega}(z),\mathbf{X})}{\partial \omega_i}\right|^3\right) < \infty$ and $\mathrm{E}\left(\left\{\frac{\partial^2 \ell(\boldsymbol{\omega}(z),\mathbf{X})}{\partial \omega_i \partial \omega_j}\right\}^2\right) < \infty$ hold for all i and j.

G. $h \to 0$, $Nh \to \infty$ and $Nh^5 = O(1)$ as $N \to \infty$.

Conditions A.–G. are mild, and they have been used in Mack & Silverman (1982), Zhou et al. (2010), Huang et al. (2013), and many others. In particular, G. is a standard condition in the literature of local-likelihood estimation such as Loader (1996, 2006) and Huang et al. (2013).

In the following theorem, we prove the asymptotic properties of the local solution $(\hat{\boldsymbol{\pi}}(z), \hat{\boldsymbol{\mu}}(z), \hat{\boldsymbol{\Theta}}(z))$ for the nonparametric finite mixture (2).

Theorem 3. *If $\lambda = O((Nh)^{-1/2})$ as $N \to \infty$, under Conditions A.–G., there exists a local maximizer $(\hat{\boldsymbol{\pi}}(z), \hat{\boldsymbol{\mu}}(z), \hat{\boldsymbol{\Theta}}(z))$ of (3) such that*

$$\sqrt{Nh}(\hat{\boldsymbol{\pi}}(z) - \boldsymbol{\pi}(z)) = O_p(1), \qquad \sqrt{Nh}(\hat{\boldsymbol{\mu}}(z) - \boldsymbol{\mu}(z)) = O_p(1),$$

and

$$\sqrt{Nh}(vec(\hat{\boldsymbol{\Theta}}(z)) - vec(\boldsymbol{\Theta}(z))) = O_p(1),$$

where $O_p(1)$ denotes the stochastic boundedness or boundedness in probability.

Remark 5. In view of Theorem 3, our proposed method delivers a nice local solution to estimate nonparametric mixing proportions $\boldsymbol{\pi}(z)$ and heterogenous graphical parameters $\boldsymbol{\mu}(z)$ and $\boldsymbol{\Theta}(z)$. In particular, when $\min_k \min_{(i,j)\in\mathcal{E}_k^z} |\theta_{kij}(z)| \gg (Nh)^{-1/2}$ is satisfied, the local maximizer $(\hat{\boldsymbol{\pi}}(z), \hat{\boldsymbol{\mu}}(z), \hat{\boldsymbol{\Theta}}(z))$ of (3) would recover all true edges and achieve the selection consistency, that is, $|\hat{\theta}_{kij}(z)| > 0$ for any k and $(i,j) \in \mathcal{E}_k^z$.

5 Simulation Studies

This section presents two simulation studies. Section 5.1 considers a nonparametric finite mixture of autoregressive (AR) and block diagonal dependencies, and Section 5.2 considers a nonparametric finite mixture of AR and random sparse dependencies. For both simulation studies, we consider $K = 2$, $\mathcal{Z} = [0, 1]$, and two mixing proportion functions:

$$\pi_1(z) = \frac{\exp(0.5z)}{1 + \exp(0.5z)} \quad \text{and} \quad \pi_2(z) = 1 - \pi_1(z).$$

We also consider different mixing probabilities $\pi_1(z) = \frac{1}{12}\cos(2\pi z) + \frac{7}{12}$ and $\pi_2(z) = 1 - \pi_1(z)$, which result in similar numerical performance. For space consideration, we only present simulation studies with logistic mixing probabilities.

We generate data at the equally spaced grid points in $\mathcal{Z}$, and generate 50 observations at each grid point. We consider dimension $p = 50, 100$. The Epanechnikov kernel is used, and the initial values are obtained by using the method of Fraley & Raftery (2002) that was implemented in the R package "mclust". To compare numerical performance, we define some average metrics over 100 replications:

- the averaged spectral norm loss: $\text{ASL} = \frac{1}{G}\sum_{z\in\mathcal{U}}\sum_{k=1}^{K} \|\hat{\boldsymbol{\Theta}}_k^z - \boldsymbol{\Theta}_k^z\|_2$.
- the averaged Frobenius norm loss: $\text{AFL} = \frac{1}{G}\sum_{z\in\mathcal{U}}\sum_{k=1}^{K} \|\hat{\boldsymbol{\Theta}}_k^z - \boldsymbol{\Theta}_k^z\|_{\text{F}}$.
- the averaged Kullback-Leibler loss: $\text{AKL} = \frac{1}{G}\sum_{z\in\mathcal{U}}\sum_{k=1}^{K} \text{KL}(\boldsymbol{\Theta}_k^{-1,z}, \hat{\boldsymbol{\Theta}}_k^{-1,z})$, where $\text{KL}(\boldsymbol{\Theta}^{-1}, \hat{\boldsymbol{\Theta}}^{-1}) = \text{tr}(\boldsymbol{\Theta}^{-1}\hat{\boldsymbol{\Theta}}) - \log|\boldsymbol{\Theta}^{-1}\hat{\boldsymbol{\Theta}}| - p$.
- the average squared error (RASE) for estimated mixing proportions:

$$\text{RASE}_\pi^2 = \frac{1}{G}\sum_{z\in\mathcal{U}}\sum_{k=1}^{K} \left(\hat{\pi}_k^z - \pi_k^z\right)^2.$$

- the average true positive rate (ATPR) and average false positive rate (AFPR):

$$\text{ATPR} = \frac{1}{G}\sum_{z\in\mathcal{U}}\frac{1}{K}\sum_{k=1}^{K}\text{TPR}_k^z \quad \text{and} \quad \text{AFPR} = \frac{1}{G}\sum_{z\in\mathcal{U}}\frac{1}{K}\sum_{k=1}^{K}\text{FPR}_k^z.$$

5.1 Mixture of AR and block diagonal dependencies

In the first simulation study, we construct the mixture of AR(1) ($\boldsymbol{\Sigma}_1^0 = 0.4^{|i-j|}$) and a two-block diagonal structure $\boldsymbol{\Theta}_2^0$ when $z = 0$. When $p = 50$ ($p = 100$), we randomly specify 25 (50) edges from the first and the second block of $\boldsymbol{\Theta}_2^0$ respectively. The corresponding entries in $\boldsymbol{\Theta}_2^0$ are uniformly generated from $[-0.2, -0.1]$ and the diagonal elements are set to be 0.25. We fix the zero mean vector and 11 equally spaced grid points. Next, we consider the smooth evolving of $\boldsymbol{\Theta}_1^z$ and $\boldsymbol{\Theta}_2^z$ at the remaining 10 grid points: we randomly add 5 (20) new edges to 1st mixture towards the AR(2) structure, and add 5 new edges to each block of 2nd mixture when $p = 50$ ($p = 100$). If necessary, we increase diagonal elements to keep the precision matrices positive definite.

First of all, we check the performance of choosing the number of mixtures using our proposed BIC criterion. We report the frequencies of $\min_\lambda$ BIC over 100 repeats. As shown in Table 1, undersmoothing in h may cause an underestimated K. Hence, we should take into account different bandwidths, instead of some given bandwidth. Our proposed $\min_{\lambda,h}$ BIC performs best in choosing correct number of mixtures.

Table 1: Performance of our proposed BIC criterion in the 1st simulation study. The true number of mixtures is $K_0 = 2$.

h	$p = 50$			$p = 100$		
	$K = 1$	$K = 2$	$K = 3$	$K = 1$	$K = 2$	$K = 3$
0.65	82	18	0	91	9	0
0.85	16	84	0	3	97	0
1.05	2	96	2	0	100	0
1.25	1	97	2	1	99	0
1.45	1	97	2	0	100	0
$\min_{\lambda,h}$ BIC	1	97	2	0	100	0

Next, we examine the performance of graphical model selection using ATPR and AFPR and of estimation using ASL, AFL, AKL and RASE$_\pi$. We compare our proposed method to Zhou et al. (2010) and Ruan et al. (2011), which are two special cases of our proposed method. The results are summarized in Tables 2 and 3. Overall, our proposed method clearly outperform two competitors, especially in terms of ATPR and estimation performance. It achieves the highest ATPR and a reasonably low AFPR. Both estimation and selection performances are less sensitive to bandwidths. Since two graphs evolves smoothly, it tends to give better result with larger bandwidth. But oversmoothing in h may lead to biased estimation of mixing proportions.

5.2 Mixture of AR and random sparse dependencies

In the second simulation study, we consider the mixture of AR(1) ($\mathbf{\Sigma}_1^0 = 0.4^{|i-j|}$) and a random sparse structure $\mathbf{\Theta}_2^0$. When $p = 50$ ($p = 100$), we set the diagonal elements of $\mathbf{\Theta}_2^0$ as 0.25 and randomly choose 55 (100) off-diagonal entries to be drawn uniformly from $[-0.25, -0.22]$. We fix the zero mean vector and 11 grid points. Here we consider the less smooth evolving of $\mathbf{\Theta}_1^z$ and $\mathbf{\Theta}_2^z$: at each of the remaining grid points, we randomly add 5 (20) new edges to both graphs

Table 2: Comparison of graphical model selection performance in the 1st simulation study.

h	$p = 50$		$p = 100$	
	ATPR	AFPR	ATPR	AFPR
Proposed Nonparametric Finite Mixture of Gaussian Graphical Models				
0.65	0.9258 (0.0113)	0.1906 (0.0011)	0.8927 (0.0090)	0.1072 (0.0006)
0.85	0.9390 (0.0116)	0.1674 (0.0011)	0.9030 (0.0104)	0.0920 (0.0005)
1.05	0.9481 (0.0112)	0.1561 (0.0011)	0.9081 (0.0105)	0.0845 (0.0005)
1.25	0.9523 (0.0107)	0.1519 (0.0010)	0.9110 (0.0098)	0.0810 (0.0006)
1.45	0.9550 (0.0103)	0.1503 (0.0010)	0.9136 (0.0094)	0.0804 (0.0005)
Simple Mixture of Gaussian Graphical Models (Ruan et al. 2011).				
-	0.8677 (0.0025)	0.0751 (0.0007)	0.6537 (0.0021)	0.0207 (0.0002)
Time Varying Gaussian Graphical Models (Zhou et al. 2010)				
0.65	0.8498 (0.0019)	0.1055 (0.0007)	0.6527 (0.0016)	0.0346 (0.0002)
0.85	0.8600 (0.0020)	0.0883 (0.0007)	0.6533 (0.0017)	0.0262 (0.0002)
1.05	0.8653 (0.0022)	0.0799 (0.0007)	0.6539 (0.0018)	0.0225 (0.0002)
1.25	0.8670 (0.0023)	0.0769 (0.0007)	0.6541 (0.0018)	0.0214 (0.0002)
1.45	0.8676 (0.0023)	0.0759 (0.0007)	0.6541 (0.0019)	0.0210 (0.0002)

Note: Ruan et al. (2011) does not involve the bandwidth selection.

and randomly remove 5 (20) existing edges when $p = 50$ ($p = 100$). If necessary, we increase diagonal elements to keep the precision matrices positive definite.

Table 4 summarizes the performance of choosing the number of mixtures. As shown in Table 4, undersmoothing in h again may cause an underestimated K. Combining different bandwidths, our proposed BIC criterion has a consistent performance in choosing the correct number of mixtures. The graphical model selection and the estimation performance are summarized in Tables 5–6. Overall, our proposed method clearly outperform two competitors. Here, both estimation and selection performances are relatively more sensitive to bandwidths. Oversmoothing in h may lead to biased estimation of both precision matrices and mixing proportions.

Based on simulation studies, our proposed method clearly outperforms Zhou et al. (2010) and Ruan et al. (2011) in the presence of nonparametric finite mixtures. The numerical evidence is consistent with theoretical properties of our proposed method.

6 A Real Application to ADHD-200 Imaging Data

This section applies our proposed method to estimate time varying brain functional connectivity from ADHD-200 Global Competition data (Biswal et al. 2010). The ADHD-200 training dataset has fMRI images, diagnosis information and other demographic variables (e.g., Age, IQ, gender,

Table 3: Comparison of graphical model estimation performance in the 1st simulation study.

p	h	ASL	AFL	AKL	RASE$_\pi$
Proposed Nonparametric Finite Mixture of Gaussian Graphical Models					
50	0.65	1.9036 (0.0290)	6.7950 (0.1320)	10.7644 (0.8102)	0.1063 (0.0052)
	0.85	1.8572 (0.0290)	6.5677 (0.1348)	9.5934 (0.8485)	0.0972 (0.0050)
	1.05	1.8442 (0.0279)	6.4717 (0.1304)	9.0155 (0.8427)	0.0988 (0.0047)
	1.25	1.8398 (0.0267)	6.4272 (0.1246)	8.7180 (0.8077)	0.0995 (0.0044)
	1.45	1.8383 (0.0259)	6.4055 (0.1205)	8.5558 (0.7809)	0.0993 (0.0041)
100	0.65	2.0519 (0.0170)	10.0884 (0.1156)	20.5775 (1.0949)	0.0668 (0.0040)
	0.85	2.0186 (0.0170)	9.9191 (0.1260)	19.3055 (1.3147)	0.0628 (0.0042)
	1.05	2.0129 (0.0170)	9.8929 (0.1299)	18.9758 (1.4092)	0.0648 (0.0039)
	1.25	2.0105 (0.0164)	9.8738 (0.1250)	18.6405 (1.3602)	0.0640 (0.0030)
	1.45	2.0091 (0.0159)	9.8648 (0.1224)	18.5014 (1.3464)	0.0667 (0.0034)
Simple Mixture of Gaussian Graphical Models (Ruan et al. 2011)					
50	-	2.3119 (0.0021)	8.6222 (0.0031)	17.8072 (0.0153)	0.6250 (0.0031)
100	-	2.5324 (0.0024)	13.1246 (0.0034)	40.8719 (0.0188)	0.6336 (0.0027)
Time Varying Gaussian Graphical Models (Zhou et al. 2010)					
50	0.65	2.2896 (0.0025)	8.5715 (0.0032)	17.7900 (0.0154)	-
	0.85	2.2948 (0.0024)	8.5825 (0.0031)	17.7274 (0.0154)	-
	1.05	2.3007 (0.0023)	8.5964 (0.0031)	17.7324 (0.0154)	-
	1.25	2.3044 (0.0022)	8.6054 (0.0031)	17.7509 (0.0153)	-
	1.45	2.3065 (0.0022)	8.6102 (0.0031)	17.7647 (0.0153)	-
100	0.65	2.5298 (0.0025)	13.0496 (0.0035)	40.6013 (0.0187)	-
	0.85	2.5297 (0.0025)	13.0743 (0.0035)	40.6280 (0.0188)	-
	1.05	2.5304 (0.0024)	13.0953 (0.0035)	40.7040 (0.0188)	-
	1.25	2.5311 (0.0024)	13.1065 (0.0034)	40.7594 (0.0188)	-
	1.45	2.5314 (0.0024)	13.1121 (0.0034)	40.7911 (0.0188)	-

Note: Zhou et al. (2010) does not estimate mixing probabilities.

Table 4: Performance of our proposed BIC criterion in the 2nd simulation study. The true number of mixtures is $K_0 = 2$.

h	$p = 50$			$p = 100$		
	$K = 1$	$K = 2$	$K = 3$	$K = 1$	$K = 2$	$K = 3$
0.65	95	5	0	100	0	0
0.85	23	77	0	5	95	0
1.05	10	89	1	1	99	0
1.25	4	94	2	0	100	0
1.45	0	97	3	0	100	0
$\min_{\lambda,h}$ BIC	0	97	3	0	100	0

Table 5: Comparison of graphical model selection performance in the 2nd simulation study.

h	$p = 50$		$p = 100$	
	ATPR	AFPR	ATPR	AFPR
Proposed Nonparametric Finite Mixture of Gaussian Graphical Models				
0.65	0.8732 (0.0160)	0.1769 (0.0011)	0.8890 (0.0113)	0.1095 (0.0005)
0.85	0.8859 (0.0177)	0.1555 (0.0013)	0.9042 (0.0118)	0.0923 (0.0005)
1.05	0.8889 (0.0183)	0.1442 (0.0014)	0.9098 (0.0118)	0.0836 (0.0006)
1.25	0.8888 (0.0184)	0.1398 (0.0014)	0.9117 (0.0115)	0.0803 (0.0006)
1.45	0.8894 (0.0185)	0.1382 (0.0014)	0.9124 (0.0113)	0.0793 (0.0006)
Simple Mixture of Gaussian Graphical Models (Ruan et al. 2011).				
-	0.8504 (0.0023)	0.0738 (0.0007)	0.6926 (0.0019)	0.0250 (0.0002)
Time Varying Gaussian Graphical Models (Zhou et al. 2010)				
0.65	0.8389 (0.0020)	0.1020 (0.0007)	0.6919 (0.0015)	0.0406 (0.0002)
0.85	0.8457 (0.0021)	0.0863 (0.0007)	0.6935 (0.0016)	0.0312 (0.0002)
1.05	0.8493 (0.0022)	0.0784 (0.0006)	0.6935 (0.0017)	0.0271 (0.0002)
1.25	0.8503 (0.0022)	0.0757 (0.0006)	0.6936 (0.0018)	0.0257 (0.0002)
1.45	0.8506 (0.0022)	0.0746 (0.0006)	0.6933 (0.0019)	0.0253 (0.0002)

Note: Ruan et al. (2011) does not involve the bandwidth selection.

handedness) of 776 subjects from 8 different sites. We focus on $N = 284$ subjects whose ages range from 9 to 13, since observed ages are not uniformly distributed outside the range 9–13. Each fMRI image has measurements for $p = 264$ seed voxels. Among these subjects, 186 subjects are typically developing controls and 98 subjects are diagnosed with ADHD. We choose Age as the covariate Z, and normalize it to $[0, 1]$. We consider three interested ages: 9, 11 and 13.

We first determine the number of mixtures by using our proposed BIC in Section 3.2. BIC is minimized when $K = 2$, which implies two heterogenous groups. Then, we estimate heterogeneous graphical models at the aforementioned interested ages respectively. Table 7 shows the estimated mixing proportions. We can see a slightly increasing trend in first mixture proportion as Age increases.

If the covariate Z is ignored, we may fail to account for heterogeneity in the ADHD-200 data. To illustrate this, we also estimate the simple mixture of Gaussian mixture models with $K = 2$. Then, we obtain that $\hat{\pi}_1 = 0.9509$ and $\hat{\pi}_2 = 0.0491$, which do not reveal any meaningful heterogeneous subpopulation. In what follows, we will investigate two heterogenous dependencies identified by our method through profiling their demographic variables, and explain their differences from three different perspectives: site information, impact of gender, and impact of IQ. We shall show that our results are supported by existing scientific findings.

Table 6: Comparison of graphical model estimation performance in the 2nd simulation study.

p	h	ASL	AFL	AKL	RASE$_\pi$
Proposed Nonparametric Finite Mixture of Gaussian Graphical Models					
50	0.65	2.1992 (0.0352)	7.4927 (0.1548)	12.7527 (0.9811)	0.1290 (0.0058)
	0.85	2.1312 (0.0362)	7.2900 (0.1646)	11.8158 (1.0693)	0.1270 (0.0060)
	1.05	2.1031 (0.0360)	7.2195 (0.1680)	11.5378 (1.1045)	0.1260 (0.0058)
	1.25	2.0973 (0.0359)	7.2041 (0.1683)	11.4536 (1.1069)	0.1261 (0.0055)
	1.45	2.0965 (0.0357)	7.2018 (0.1682)	11.4282 (1.1064)	0.1264 (0.0054)
100	0.65	2.2518 (0.0201)	10.0592 (0.1270)	20.0166 (1.1550)	0.0695 (0.0047)
	0.85	2.2053 (0.0186)	9.8330 (0.1261)	18.2240 (1.2288)	0.0595 (0.0046)
	1.05	2.1981 (0.0174)	9.7937 (0.1237)	17.7696 (1.2573)	0.0599 (0.0038)
	1.25	2.2014 (0.0169)	9.7985 (0.1221)	17.6933 (1.2571)	0.0621 (0.0034)
	1.45	2.2039 (0.0166)	9.8037 (0.1209)	17.6861 (1.2501)	0.0647 (0.0034)
Simple Mixture of Gaussian Graphical Models (Ruan et al. 2011)					
50	-	2.6246 (0.0028)	8.8763 (0.0045)	16.0568 (0.0146)	0.6264 (0.0029)
100	-	2.7834 (0.0022)	13.0387 (0.0038)	36.7745 (0.0173)	0.6287 (0.0028)
Time Varying Gaussian Graphical Models (Zhou et al. 2010)					
50	0.65	2.6187 (0.0028)	8.8399 (0.0046)	16.1026 (0.0148)	-
	0.85	2.6203 (0.0028)	8.8517 (0.0046)	16.0414 (0.0149)	-
	1.05	2.6220 (0.0028)	8.8619 (0.0046)	16.0298 (0.0149)	-
	1.25	2.6230 (0.0028)	8.8674 (0.0046)	16.0337 (0.0148)	-
	1.45	2.6235 (0.0028)	8.8702 (0.0046)	16.0386 (0.0148)	-
100	0.65	2.7776 (0.0023)	12.9454 (0.0037)	36.3898 (0.0169)	-
	0.85	2.7781 (0.0022)	12.9779 (0.0038)	36.4454 (0.0172)	-
	1.05	2.7798 (0.0022)	13.0040 (0.0038)	36.5506 (0.0172)	-
	1.25	2.7810 (0.0022)	13.0178 (0.0038)	36.6256 (0.0172)	-
	1.45	2.7817 (0.0022)	13.0244 (0.0038)	36.6678 (0.0173)	-

Note: Zhou et al. (2010) does not estimate mixing probabilities.

Table 7: Estimated mixing proportions at Age 9, 11 and 13.

	Age 9	Age 11	Age 13
$\hat{\pi}_1$	0.6742	0.6870	0.7011
$\hat{\pi}_2$	0.3258	0.3130	0.2989

Firstly, we explore how subpopulations are composed with subjects from various sites. As shown in Figure 2, both mixtures are formed with subjects from heterogeneous locations. This confirms the previous study that geographic locations are not sufficient to explain variability of ADHD (Polanczyk et al. 2007). Hence we need to further investigate their individual commonality beyond geographic locations.

Figure 2: Site information: 1st mixture (left panel) and 2nd mixture (right panel).

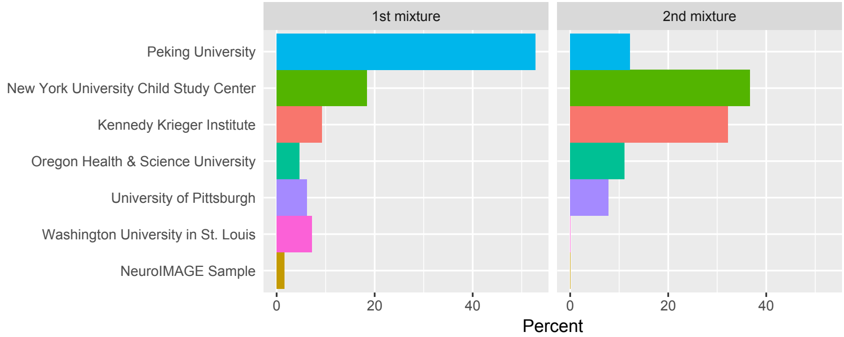

Secondly, we study the relationship between gender and ADHD status (i.e., whether the subject has ADHD or not). In the existing literature, gender difference in ADHD is an important research topic (Arnold 1996). There are two main arguments about the reason why the boys are more likely to be diagnosed with ADHD than girls. On one hand, some researchers insist that there is actually gender difference in ADHD. On the other hand, other studies show that there are other issues for example, other demographic covariates or the bias of the diagnose test that affects diagnose results. Here, we test the independence between gender and ADHD status in two mixture respectively. Their corresponding contingency tables are given in Table 8. For the first mixture, we compute the chi-square test statistic, $\chi^2 = 7.3106$ with associated p-value = 0.0069. It implies that there is an indeed relationship between gender and ADHD status in this mixture. While for the second mixture, we have chi-square test statistic, $\chi^2 = 0.5237$ with associate p-value = 0.4693, which indicates that gender and ADHD status could be independent in the second mixture. Therefore, we successfully identify two heterogeneous subpopulations: the first one is consistent with the previous study that ADHD is diagnosed at a significantly higher rate in boys than in girls (Sauver et al. 2004); the second one is consistent with another study that there may exist other covariates strongly related to the ADHD, but which are not different for boys and girls so that ADHD are not systematically different for boys and girls (Bauermeister et al. 2007). Both subpopulations support their corresponding scientific findings respectively.

Thirdly, we investigate the full scale IQ scores for both mixtures. Table 9 summarizes the

Table 8: Contingency tables with gender and whether they have ADHD or not. 1st mixture (left table) and 2nd mixture (right table).

	Male	Female	Total
Control	77	57	134
ADHD	48	13	61
Total	125	70	195

	Male	Female	Total
Control	30	22	52
ADHD	25	12	37
Total	55	34	89

average full scale IQ for each mixture. For the first mixture, we can clearly see typically developing children have a higher average IQ score than the children with ADHD: female control's average IQ is 16 higher than female ADHD's average IQ, and male control's average IQ is 12.32 higher than male ADHD's average IQ. This result shows that full scale IQ scores are reliably different between individuals with ADHD and typically developing controls in the first mixture, which is consistent with Frazier et al. (2004), García-Sánchez et al. (1997). However, the second mixture exhibits a very different aspect: typically developing children in the second mixture have a lower average IQ score compared to those in the first mixture, while ADHD children in the second mixture have a higher average IQ score than those in the first mixture. Therefore, there is only no significant difference in terms of average IQ between typically growing children and children with ADHD in the second mixture: female control's average IQ is 7.77 higher than female ADHD's average IQ, and male control's average IQ is 4.30 higher than male ADHD's average IQ. Based on the full scale IQ, these two heterogeneous mixtures further justifies the power of our proposed method.

Table 9: Average full scale IQ scores for both mixtures.

	1st mixture	2nd mixture
Male Control	118.85	112.30
Female Control	115.54	111.77
Male ADHD	106.53	108.00
Female ADHD	99.54	104.00

7 Acknowledgement

The authors thank the Editor, an associate editor, and two referees for their constructive comments and suggestions. Lingzhou Xue's research is partially supported by the National Science Foundation grant DMS-1505256.

8 Appendix

8.1 Technical details for Section 3.1

We include some technical details for updating mixing proportions (7) and graphical parameters (8) and (9) in our proposed EM algorithm.

8.1.1 Solving mixing proportions (7)

In order to solve (5), we introduce Lagrange multiplier α with respect to the constraint $\sum_{k=1}^{K} \pi_k^z = 1$, and consider the following first-order optimality equation

$$\frac{\partial}{\partial \pi_k^z}\left[\frac{1}{N}\sum_{n=1}^{N}\sum_{k=1}^{K}\gamma_{kn}^{(t+1)}\log \pi_k^z K_h(z_n - z) + \alpha\left(\sum_{k=1}^{K}\pi_k^z - 1\right)\right] = 0,$$

which can be further simplified as

$$\frac{1}{N}\sum_{n=1}^{N}\gamma_{kn}^{(t+1)}\frac{1}{\pi_k^z}K_h(z_n - z) + \alpha = 0.$$

From the above equation, we immediately obtain

$$\pi_k^z = -\frac{1}{\alpha N}\sum_{n=1}^{N}\gamma_{kn}^{(t+1)}K_h(z_n - z).$$

Then, it is easy to solve $\alpha = -\frac{1}{N}\sum_{n=1}^{N} K_h(z_n - z)$ from

$$\sum_{k=1}^{K}\pi_k^z - 1 = -\frac{1}{\alpha N}\sum_{n=1}^{N}K_h(z_n - z) - 1 = 0$$

Therefore, we obtain the mixing proportions (7):

$$\pi_k^{z(t+1)} = \frac{\sum_{n=1}^{N}\gamma_{kn}^{(t+1)}K_h(z_n - z)}{\sum_{n=1}^{N}K_h(z_n - z)}.$$

8.1.2 Solving graphical parameters (8) and (9)

First we solve (6) to obtain the update of $\boldsymbol{\mu}_k^z$. To this end, we consider the following first-order optimality equation

$$\frac{\partial}{\partial \boldsymbol{\mu}_k^z}\left[\frac{1}{N}\sum_{n=1}^{N}\gamma_{kn}^{(t+1)}\left(\frac{1}{2}\log|\boldsymbol{\Theta}_k^z| - \frac{1}{2}(\mathbf{x}_n - \boldsymbol{\mu}_k^z)'\boldsymbol{\Theta}_k^z(\mathbf{x}_n - \boldsymbol{\mu}_k^z)\right)K_h(z_n - z)\right] = 0$$

which can be further simplified as

$$\frac{1}{N}\sum_{n=1}^{N}\gamma_{kn}^{(t+1)}(\mathbf{x}_n-\boldsymbol{\mu}_k^z)K_h(z_n-z)=0$$

Thus, we simply solve the above equation to obtain (8):

$$\boldsymbol{\mu}_k^{z(t+1)}=\frac{\sum_{n=1}^{N}\gamma_{kn}^{(t+1)}K_h(z_n-z)\mathbf{x}_n}{\sum_{n=1}^{N}\gamma_{kn}^{(t+1)}K_h(z_n-z)}.$$

After obtaining $\boldsymbol{\mu}_k^{z(t+1)}$, we only need to solve $\boldsymbol{\Theta}_k^{z(t+1)}$ from

$$\frac{1}{N}\sum_{n=1}^{N}\gamma_{kn}^{(t+1)}\left(\frac{1}{2}\log|\boldsymbol{\Theta}_k^z|-\frac{1}{2}(\mathbf{x}_n-\boldsymbol{\mu}_k^{z(t+1)})'\boldsymbol{\Theta}_k^z(\mathbf{x}_n-\boldsymbol{\mu}_k^{z(t+1)})\right)K_h(z_n-z)-\lambda\|\boldsymbol{\Theta}_k^z\|_1.$$

Let $a_k^{(t+1)}=\sum_{n=1}^{N}\gamma_{kn}^{(t+1)}K_h(z_n-z)$ and

$$A_k^{(t+1)}=\sum_{n=1}^{N}\gamma_{kn}^{(t+1)}K_h(z_n-z)(\mathbf{x}_n-\boldsymbol{\mu}_k^{z(t+1)})(\mathbf{x}_n-\boldsymbol{\mu}_k^{z(t+1)})'.$$

Now we can rewrite the above equation as

$$\frac{1}{2N}a_k^{(t+1)}\log|\boldsymbol{\Theta}_k^z|-\frac{1}{2N}\mathrm{tr}\left(\boldsymbol{\Theta}_k^zA_k^{(t+1)}\right)-\lambda\|\boldsymbol{\Theta}_k^z\|_1.$$

Thus, we solve the graphical parameter (9) from the following ℓ_1 penalized log-determinant problem

$$\boldsymbol{\Theta}_k^{z(t+1)}=\arg\max_{\boldsymbol{\Theta}_k^z}\left\{\log|\boldsymbol{\Theta}_k^z|-\mathrm{tr}(\boldsymbol{\Theta}_k^z\mathbf{A}_k^{z(t+1)})-\lambda_1\|\boldsymbol{\Theta}_k^z\|_1\right\},$$

where $\lambda_1=2N\lambda/a_k^{(t+1)}$ and

$$\mathbf{A}_k^{z(t+1)}=\frac{A_k^{(t+1)}}{a_k^{(t+1)}}=\frac{\sum_{n=1}^{N}\gamma_{kn}^{(t+1)}K_h(z_n-z)(\mathbf{x}_n-\boldsymbol{\mu}_k^{z(t+1)})(\mathbf{x}_n-\boldsymbol{\mu}_k^{z(t+1)})'}{\sum_{n=1}^{N}\gamma_{kn}^{(t+1)}K_h(z_n-z)}.$$

By abuse of notation, we continue to write λ_1 as λ throughout this paper.

8.2 Proof of Theorem 1

Proof. In the first part, we prove the ascent property. Assume that the unobserved data $(c_n, n=1,\dots,N)$ are random samples from population $\mathcal{C}$. Then, the complete data $\{(\mathbf{x}_n,z_n,c_n),n=1,\dots,N\}$ are random samples from $(\mathbf{X},Z,\mathcal{C})$. Let $f(z)$ be the marginal density of Z. The conditional probability of $\mathcal{C} = k$ given $\mathbf{x}$, $\boldsymbol{\pi}^z$, $\boldsymbol{\mu}^z$, and $\boldsymbol{\Theta}^z$ is

$$g(k \mid \mathbf{x}, \boldsymbol{\pi}^z, \boldsymbol{\mu}^z, \boldsymbol{\Theta}^z) = \frac{\pi_k^z \phi(\mathbf{x} \mid \boldsymbol{\mu}_k^z, \boldsymbol{\Theta}_k^z)}{\sum_{k=1}^{k} \pi_k^z \phi(\mathbf{x} \mid \boldsymbol{\mu}_k^z, \boldsymbol{\Theta}_k^z)}. \tag{10}$$

For given $\boldsymbol{\pi}^{(t)}(z_n)$, $\boldsymbol{\mu}^{(t)}(z_n)$, and $\boldsymbol{\Theta}^{(t)}(z_n)$, we have

$$\sum_{k=1}^{K} g(k \mid \mathbf{x}_n, \boldsymbol{\pi}^{(t)}(z_n), \boldsymbol{\mu}^{(t)}(z_n), \boldsymbol{\Theta}^{(t)}(z_n)) = \sum_{k=1}^{K} \gamma_{kn}^{(t+1)} = 1, \tag{11}$$

for $n = 1, \ldots, N$. Using (11) we can rewrite the ℓ_1-penalized local log-likelihood as

$$\mathcal{L}_z(\boldsymbol{\pi}^z, \boldsymbol{\mu}^z, \boldsymbol{\Theta}^z) = \frac{1}{N} \sum_{n=1}^{N} \left[\sum_{k=1}^{K} \log \left(\sum_{k=1}^{K} \pi_k^z \phi(\mathbf{x_n} \mid \boldsymbol{\mu}_k^z, \boldsymbol{\Theta}_k^z) \right) \gamma_{kn}^{(t+1)} \right] K_h(z_n - z) - \lambda \sum_{k=1}^{K} \|\boldsymbol{\Theta}_k^z\|_1. \tag{12}$$

Now (12) can be separated into two parts using (10),

$$\mathcal{L}_z(\boldsymbol{\pi}^z, \boldsymbol{\mu}^z, \boldsymbol{\Theta}^z) = Q(\boldsymbol{\pi}^z, \boldsymbol{\mu}^z, \boldsymbol{\Theta}^z) - H(\boldsymbol{\pi}^z, \boldsymbol{\mu}^z, \boldsymbol{\Theta}^z)$$

where

$$Q(\boldsymbol{\pi}^z, \boldsymbol{\mu}^z, \boldsymbol{\Theta}^z) = \frac{1}{N} \sum_{n=1}^{N} \left[\sum_{k=1}^{K} \log \left(\pi_k^z \phi(\mathbf{x_n} \mid \boldsymbol{\mu}_k^z, \boldsymbol{\Theta}_k^z) \right) \gamma_{kn}^{(t+1)} \right] K_h(z_n - z) - \lambda \sum_{k=1}^{K} \|\boldsymbol{\Theta}_k^z\|_1$$

and

$$H(\boldsymbol{\pi}^z, \boldsymbol{\mu}^z, \boldsymbol{\Theta}^z) = \frac{1}{N} \sum_{n=1}^{N} \left[\sum_{k=1}^{K} \log \left(g(k \mid \mathbf{x}_n, \boldsymbol{\pi}^z, \boldsymbol{\mu}^z, \boldsymbol{\Theta}^z) \right) \gamma_{kn}^{(t+1)} \right] K_h(z_n - z).$$

Thus, the difference between ℓ_1-penalized local log-likelihood at the updated estimates and at the current estimates can be written as,

$$\begin{aligned} &\mathcal{L}_z(\boldsymbol{\pi}^{z(t+1)}, \boldsymbol{\mu}^{z(t+1)}, \boldsymbol{\Theta}^{z(t+1)}) - \mathcal{L}_z(\boldsymbol{\pi}^{z(t)}, \boldsymbol{\mu}^{z(t)}, \boldsymbol{\Theta}^{z(t)}) \\ =&Q(\boldsymbol{\pi}^{z(t+1)}, \boldsymbol{\mu}^{z(t+1)}, \boldsymbol{\Theta}^{z(t+1)}) - Q(\boldsymbol{\pi}^{z(t)}, \boldsymbol{\mu}^{z(t)}, \boldsymbol{\Theta}^{z(t)}) \\ &- \left(\frac{1}{N} \sum_{n=1}^{N} \left[\sum_{k=1}^{K} \log \left(\frac{g(k \mid \mathbf{x}_n, \boldsymbol{\pi}^{z(t+1)}, \boldsymbol{\mu}^{z(t+1)}, \boldsymbol{\Theta}^{z(t+1)})}{g(k \mid \mathbf{x}_n, \boldsymbol{\pi}^{z(t)}, \boldsymbol{\mu}^{z(t)}, \boldsymbol{\Theta}^{z(t)})} \right) \gamma_{kn}^{(t+1)} \right] K_h(z_n - z) \right). \end{aligned}$$

In the M-step, we update $\boldsymbol{\pi}^{z(t+1)}$, $\boldsymbol{\mu}^{z(t+1)}$, and $\boldsymbol{\Theta}^{z(t+1)}$ such that

$$Q(\boldsymbol{\pi}^{z(t+1)}, \boldsymbol{\mu}^{z(t+1)}, \boldsymbol{\Theta}^{z(t+1)}) \geq Q(\boldsymbol{\pi}^{z(t)}, \boldsymbol{\mu}^{z(t)}, \boldsymbol{\Theta}^{z(t)}). \tag{13}$$

Hence, using (13) we now have,

$$\begin{aligned}&\mathcal{L}_z(\boldsymbol{\pi}^{z(t+1)}, \boldsymbol{\mu}^{z(t+1)}, \boldsymbol{\Theta}^{z(t+1)}) - \mathcal{L}_z(\boldsymbol{\pi}^{z(t)}, \boldsymbol{\mu}^{z(t)}, \boldsymbol{\Theta}^{z(t)})\\ &\geq -\frac{1}{N}\sum_{n=1}^{N}\left[\sum_{k=1}^{K}\log\left(\frac{g(k \mid \mathbf{x}_n, \boldsymbol{\pi}^{z(t+1)}, \boldsymbol{\mu}^{z(t+1)}, \boldsymbol{\Theta}^{z(t+1)})}{g(k \mid \mathbf{x}_n, \boldsymbol{\pi}^{z(t)}, \boldsymbol{\mu}^{z(t)}, \boldsymbol{\Theta}^{z(t)})}\right)\gamma_{kn}^{(t+1)}\right]K_h(z_n - z).\end{aligned}$$

Now to show

$$\liminf_{N\to\infty}\left[\mathcal{L}_z(\boldsymbol{\pi}^{z(t+1)}, \boldsymbol{\mu}^{z(t+1)}, \boldsymbol{\Theta}^{z(t+1)}) - \mathcal{L}_z(\boldsymbol{\pi}^{z(t)}, \boldsymbol{\mu}^{z(t)}, \boldsymbol{\Theta}^{z(t)})\right] \geq 0,$$

is equivalent to show

$$\limsup_{N\to\infty}\frac{1}{N}\sum_{n=1}^{N}\left[\sum_{k=1}^{K}\log\left(\frac{g(k \mid \mathbf{x}_n, \boldsymbol{\pi}^{z(t+1)}, \boldsymbol{\mu}^{z(t+1)}, \boldsymbol{\Theta}^{z(t+1)})}{g(k \mid \mathbf{x}_n, \boldsymbol{\pi}^{z(t)}, \boldsymbol{\mu}^{z(t)}, \boldsymbol{\Theta}^{z(t)})}\right)\gamma_{kn}^{(t+1)}\right]K_h(z_n - z) \leq 0.$$

Let,

$$L_N(z) = \frac{1}{N}\sum_{n=1}^{N}\varphi(\mathbf{x}_n, z_n)K_h(z_n - z)$$

where

$$\varphi(\mathbf{x}_n, z_n) = \sum_{k=1}^{K}\log\left(\frac{g(k \mid \mathbf{x}_n, \boldsymbol{\pi}^{z(t+1)}, \boldsymbol{\mu}^{z(t+1)}, \boldsymbol{\Theta}^{z(t+1)})}{g(k \mid \mathbf{x}_n, \boldsymbol{\pi}^{z(t)}, \boldsymbol{\mu}^{z(t)}, \boldsymbol{\Theta}^{z(t)})}\right)g(k \mid \mathbf{x}_n, \boldsymbol{\pi}^{(t)}(z_n), \boldsymbol{\mu}^{(t)}(z_n), \boldsymbol{\Theta}^{(t)}(z_n)).$$

To apply Theorem A by Mack & Silverman (1982) we just need to make sure two conditions (C1) and (C2) are satisfied.

By conditions A. and B., we know $g(k \mid \mathbf{X}, \boldsymbol{\pi}^{(t)}(Z), \boldsymbol{\mu}^{(t)}(Z), \boldsymbol{\Theta}^{(t)}(Z))$ is continuous function of z and the support of Z is closed and bounded. Hence by applying Boundness theorem, we have $1 \geq g(k \mid \mathbf{X}, \boldsymbol{\pi}^{(t)}(Z), \boldsymbol{\mu}^{(t)}(Z), \boldsymbol{\Theta}^{(t)}(Z)) \geq a > 0$ for some small value a, and using Young's inequality we can prove $\mathrm{E}\{\varphi(\mathbf{X},Z)^2\}<\infty$ which satisfies the condition (C2) of Theorem A.

$$\begin{aligned}
&\mathrm{E}\left(\sum_{k=1}^{K}\left(\log\frac{g(k\mid\mathbf{X},\boldsymbol{\pi}^{z(t+1)},\boldsymbol{\mu}^{z(t+1)},\boldsymbol{\Theta}^{z(t+1)})}{g(k\mid\mathbf{X},\boldsymbol{\pi}^{z(t)},\boldsymbol{\mu}^{z(t)},\boldsymbol{\Theta}^{z(t)})}\right)g(k|\mathbf{X},\boldsymbol{\pi}^{(t)}(Z),\boldsymbol{\mu}^{(t)}(Z),\boldsymbol{\Theta}^{(t)}(Z))\right)^2\\
\leq&K\sum_{k=1}^{K}\mathrm{E}\left(\left(\log\frac{g(k\mid\mathbf{X},\boldsymbol{\pi}^{z(t+1)},\boldsymbol{\mu}^{z(t+1)},\boldsymbol{\Theta}^{z(t+1)})}{g(k\mid\mathbf{X},\boldsymbol{\pi}^{z(t)},\boldsymbol{\mu}^{z(t)},\boldsymbol{\Theta}^{z(t)})}\right)g(k|\mathbf{X},\boldsymbol{\pi}^{(t)}(Z),\boldsymbol{\mu}^{(t)}(Z),\boldsymbol{\Theta}^{(t)}(Z))\right)^2\\
\leq&2K\sum_{k=1}^{K}\left((\log g(k\mid\mathbf{X},\boldsymbol{\pi}^{z(t+1)},\boldsymbol{\mu}^{z(t+1)},\boldsymbol{\Theta}^{z(t+1)}))^2+(\log g(k\mid\mathbf{X},\boldsymbol{\pi}^{z(t)},\boldsymbol{\mu}^{z(t)},\boldsymbol{\Theta}^{z(t)}))^2\right)\\
\leq&4K\sum_{k=1}^{K}|\log a|^2\\
=&4K^2|\log a|^2<\infty
\end{aligned}$$

Also, by condition D. with Cauchy-Schwarz inequality and bounded support, condition (C1) of Theorem A is satisfied. Now by using Theorem A, we have

$$\sup_{J}|L_N(z)-f(z)\mathrm{E}\varphi(\mathbf{X},z)|=o(1)\quad\text{w.p.1.}$$

where J is a compact interval on which the density of Z is bounded from 0. The proof follows from

$$\begin{aligned}
&\mathrm{E}\varphi(\mathbf{X},z)\\
=&\ \mathrm{E}\left[\sum_{k=1}^{K}\log\left(\frac{g(k\mid\mathbf{X},\boldsymbol{\pi}^{z(t+1)},\boldsymbol{\mu}^{z(t+1)},\boldsymbol{\Theta}^{z(t+1)})}{g(k|\mathbf{X},\boldsymbol{\pi}^{z(t)},\boldsymbol{\mu}^{z(t)},\boldsymbol{\Theta}^{z(t)})}\right)g(k\mid\mathbf{X},\boldsymbol{\pi}^{z(t)},\boldsymbol{\mu}^{z(t)},\boldsymbol{\Theta}^{z(t)})\right]\\
\leq&\ \mathrm{E}\left(\log\left[\sum_{k=1}^{K}\left(\frac{g(k\mid\mathbf{X},\boldsymbol{\pi}^{z(t+1)},\boldsymbol{\mu}^{z(t+1)},\boldsymbol{\Theta}^{z(t+1)})}{g(k\mid\mathbf{X},\boldsymbol{\pi}^{z(t)},\boldsymbol{\mu}^{z(t)},\boldsymbol{\Theta}^{z(t)})}\right)g(k\mid\mathbf{X},\boldsymbol{\pi}^{z(t)},\boldsymbol{\mu}^{z(t)},\boldsymbol{\Theta}^{z(t)})\right]\right)\\
=&\ 0
\end{aligned}$$

by Jensen's inequality.

Now, we prove that $\{\mathcal{L}_z(\boldsymbol{\pi}^{z(t)},\boldsymbol{\mu}^{z(t)},\boldsymbol{\Theta}^{z(t)}):\ t=0,1,2,\ldots\}$ increases monotonically to some value $\bar{\mathcal{L}}<\infty$ in the second part. Given the ascent property in the first part, it remains to prove that $\mathcal{L}_z(\boldsymbol{\pi}^z,\boldsymbol{\mu}^z,\boldsymbol{\Theta}^z)$ is bounded from above. To this end, we consider

$$\exp(N\mathcal{L}_z(\boldsymbol{\pi}^z,\boldsymbol{\mu}^z,\boldsymbol{\Theta}^z))=\prod_{n=1}^{N}\left\{\left(\sum_{k=1}^{K}\pi_k^z\phi(\mathbf{x}_n|\boldsymbol{\mu}_k^z,\boldsymbol{\Theta}_k^z)\right)^{K_h(z_n-z)}\prod_{k=1}^{K}\exp\left(-\lambda\|\boldsymbol{\Theta}_k^z\|_1\right)\right\}.$$

It is equivalent to show that $\exp(N\mathcal{L}_z(\boldsymbol{\pi}^z, \boldsymbol{\mu}^z, \boldsymbol{\Theta}^z))$ is bounded from above. Given that

$$\phi(\mathbf{x}_n|\boldsymbol{\mu}_k^z, \boldsymbol{\Theta}_k^z) = (2\pi)^{-p/2}|\boldsymbol{\Theta}_k^z|^{1/2}\exp\left(-\frac{1}{2}(\mathbf{x}_n - \boldsymbol{\mu}_k^z)'\boldsymbol{\Theta}_k^z(\mathbf{x}_n - \boldsymbol{\mu}_k^z)\right)$$

and $\boldsymbol{\Theta}_k^z$ is positive definite, we only need to handle the unboundedness issue of $|\boldsymbol{\Theta}_k^z|^{1/2}$ when $|\boldsymbol{\Theta}_k^z| \to \infty$. But note that, with the penalty term $\exp(-\lambda\|\boldsymbol{\Theta}_k^z\|_1)$, $\exp(N\mathcal{L}_z(\boldsymbol{\pi}^z, \boldsymbol{\mu}^z, \boldsymbol{\Theta}^z))$ would tend to 0 when $|\boldsymbol{\Theta}_k^z| \to \infty$ for any k. Thus, $\mathcal{L}_z(\boldsymbol{\pi}^z, \boldsymbol{\mu}^z, \boldsymbol{\Theta}^z)$ is bounded from above. It follows that $\{\mathcal{L}_z(\boldsymbol{\pi}^{z(t)}, \boldsymbol{\mu}^{z(t)}, \boldsymbol{\Theta}^{z(t)}) : \ t = 0, 1, 2, \ldots\}$ increases monotonically to some value $\bar{\mathcal{L}} < \infty$ with probability tending to 1. It completes the proof of Theorem 1. □

8.3 Proof of Theorem 2

Proof. To simplify notation, let $\boldsymbol{\omega}^z = (\boldsymbol{\pi}^z, \boldsymbol{\mu}^z, \boldsymbol{\Theta}^z)$. Recall that $\boldsymbol{\omega}^{z(t)}$ is the sequence generated by the proposed algorithm. We need to prove that every cluster point $\bar{\boldsymbol{\omega}}$ is a stationary point of $\mathcal{L}_z(\boldsymbol{\omega}^z)$, where there exists a convergent subsequence $\boldsymbol{\omega}^{z(t_j)} \to \bar{\boldsymbol{\omega}}$.

Similar to the proof of Theorem 1, the local penalized log-likelihood can be written as $\mathcal{L}_z(\boldsymbol{\omega}^z) = Q(\boldsymbol{\omega}^z) - H(\boldsymbol{\omega}^z)$. By Theorem 1, with probability tending to 1, we have the following relationship:

$$H(\boldsymbol{\omega}^{z(t+1)}) \leq H(\boldsymbol{\omega}^{z(t)}). \tag{14}$$

Note that $Q(\boldsymbol{\omega}^z)$ and $H(\boldsymbol{\omega}^z)$ are continuous functions. Furthermore, $Q(\boldsymbol{\omega}^z)$ is a convex function of $\boldsymbol{\omega}^z$ and strictly convex in each coordinate of $\boldsymbol{\omega}^z$.

Now, we take the directional derivative of $\mathcal{L}_z(\boldsymbol{\omega}^z)$ to obtain

$$\mathcal{L}_z(\bar{\boldsymbol{\omega}}^z; d) = Q'(\bar{\boldsymbol{\omega}}^z; d) - < \bigtriangledown H(\bar{\boldsymbol{\omega}}^z), d > .$$

Next we want to show $\mathcal{L}_z(\bar{\boldsymbol{\omega}}^z; d) \leq 0$. Note that $\bigtriangledown H(\bar{\boldsymbol{\omega}}^z) = 0$ as $H(\cdot)$ is maximized for $\bar{\boldsymbol{\omega}}^z$. Hence it remains to show that $Q'(\bar{\boldsymbol{\omega}}^z; d) \leq 0$ for all directions d. As in our proposed algorithm, we have

$$Q(\boldsymbol{\omega}^{z(t)}) \leq Q(\boldsymbol{\omega}^{z(t+1)}).$$

In addition, by Theorem 1, for any given point z and $t = 0, 1, 2 \ldots$, with probability tending to 1, we have

$$\mathcal{L}_z(\boldsymbol{\omega}^{z(t)}) \leq \mathcal{L}_z(\boldsymbol{\omega}^{z(t+1)}). \tag{15}$$

Equation (15) and the converging subsequence imply that the sequence $\{\mathcal{L}_z(\boldsymbol{\omega}^{z(t)}); t = 0, 1, 2, \ldots\}$

converges to $\mathcal{L}_z(\bar{\boldsymbol{\omega}}^z)$. Now, using (14) and the fact that $\{\mathcal{L}_z(\boldsymbol{\omega}^{z(t)}); t = 0, 1, 2, \ldots\}$ converges to $\mathcal{L}_z(\bar{\boldsymbol{\omega}}^z)$ we have,

$$
\begin{aligned}
0 &\leq Q(\boldsymbol{\omega}^{z(t+1)}) - Q(\boldsymbol{\omega}^{z(t)}) \\
&= \mathcal{L}_z(\boldsymbol{\omega}^{z(t+1)}) - \mathcal{L}_z(\boldsymbol{\omega}^{z(t)}) + H(\boldsymbol{\omega}^{z(t+1)}) - H(\boldsymbol{\omega}^{z(t)}) \\
&\leq \mathcal{L}_z(\boldsymbol{\omega}^{z(t+1)}) - \mathcal{L}_z(\boldsymbol{\omega}^{z(t)}) \to 0.
\end{aligned}
$$

Therefore, we conclude that the sequence $\{Q(\boldsymbol{\omega}^{z(t+1)}) - Q(\boldsymbol{\omega}^{z(t)}); t = 0, 1, 2, \ldots\}$ converges to zero with probability tending to 1.

The remaining part of the proof follows from the proof of Theorem 6 in Städler et al. (2010). We can show that $\bar{\boldsymbol{\omega}}^z$ is a coordinate-wise maximum. By following Tseng (2001), $\bar{\boldsymbol{\omega}}^z$ is shown to be a stationary point of $Q(\cdot)$ so that $Q'(\bar{\boldsymbol{\omega}}^z; d) \leq 0$ for all directions d. This completes the proof of Theorem 2. □

8.4 Proof of Theorem 3

Proof. Note that we can also write $\boldsymbol{\omega}(z) = (\boldsymbol{\pi}(z), \boldsymbol{\mu}(z), \boldsymbol{\Theta}(z))$ in following vector form,

$$
(\boldsymbol{\pi}(z), \boldsymbol{\mu}(z), \theta_{11}(z), \ldots, \theta_{1p}(z), (\theta_{1ij}(z))_{1\leq i<j\leq p}, \ldots, \theta_{K1}(z), \ldots, \theta_{Kp}(z), (\theta_{Kij}(z))_{1\leq i<j\leq p}).
$$

For ease of notations, we introduce the following notations:

$$
q_1(\boldsymbol{\omega}(z), \mathbf{x}) = \frac{\partial \ell(\boldsymbol{\omega}(z), \mathbf{x})}{\partial \boldsymbol{\omega}}, \quad q_2(\boldsymbol{\omega}(z), \mathbf{x}) = \frac{\partial^2 \ell(\boldsymbol{\omega}(z), \mathbf{x})}{\partial \boldsymbol{\omega} \partial \boldsymbol{\omega}^T},
$$

$$
I(z) = -\mathrm{E}\left[q_2(\boldsymbol{\omega}(Z), \mathbf{X}) \mid Z = z\right],
$$

$$
\Lambda(u \mid z) = \int_{X_p} \cdots \int_{X_1} q_1(\boldsymbol{\omega}(z), \mathbf{x}) \eta(\mathbf{x} \mid \boldsymbol{\omega}(u))\, dx_1 \cdots dx_p,
$$

$$
\ell(\boldsymbol{\omega}(z), \mathbf{x}) = \log \sum_{k=1}^{K} \pi_k(z) \phi(\mathbf{x} \mid \boldsymbol{\mu}_k(z), \boldsymbol{\Theta}_k(z)) \quad (:= \log \eta(\mathbf{x}|\boldsymbol{\omega}(z))),
$$

$$
\mathcal{L}(\boldsymbol{\omega}(z)) = h \sum_{n=1}^{N} \ell(\boldsymbol{\omega}(z), \mathbf{x}_n) K_h(z_n - z) - Nh\lambda \sum_{k=1}^{K} \sum_{j \neq q} |\theta_{kjq}(z)|.
$$

We also cite the following lemma from Lemma 1 of Huang et al. (2013).

Lemma 1. *Under condition A., E. and F., for any interior point z of $\mathcal{Z}$ it holds that*

$$\begin{aligned} &\mathrm{E}[q_1(\boldsymbol{\omega}(Z), \mathbf{X}) \mid Z = z] = 0 \\ &\mathrm{E}[q_2(\boldsymbol{\omega}(Z), \mathbf{X}) \mid Z = z] = -\mathrm{E}[q_1(\boldsymbol{\omega}(Z), \mathbf{X}) q_1^T(\boldsymbol{\omega}(Z), \mathbf{X}) \mid Z = z) \end{aligned}$$

Let $\alpha = (Nh)^{-1/2}$. Now we want to show that for any given $\varepsilon > 0$, there exists a large constant C such that

$$P\left(\sup_{\|\mathbf{u}\|=C} \mathcal{L}(\boldsymbol{\omega}(z) + \alpha\mathbf{u}) < \mathcal{L}(\boldsymbol{\omega}(z))\right) \geq 1 - \varepsilon.$$

This implies that with probability at least $1 - \varepsilon$, there exists a local maximum in the ball $\{\boldsymbol{\omega}(z) + \alpha\mathbf{u} : \|\mathbf{u}\| \leq C\}$. Hence, there exists a local maximizer such that $(\hat{\boldsymbol{\omega}}(z) - \boldsymbol{\omega}(z)) = O_p((Nh)^{-1/2})$.

Now we define,

$$\begin{aligned} D(\mathbf{u}) =& \mathcal{L}(\boldsymbol{\omega}(z) + \alpha\mathbf{u}) - \mathcal{L}(\boldsymbol{\omega}(z)) \\ \leq& h\sum_{n=1}^{N} (\ell(\boldsymbol{\omega}(z) + \alpha\mathbf{u}, \mathbf{x}_n) - \ell(\boldsymbol{\omega}(z), \mathbf{x}_n)) K_h(z_n - z) \\ &- Nh\lambda \sum_{k=1}^{K} \sum_{j\neq q}^{s_k} \{|\theta_{kjq}(z) + \alpha u| - |\theta_{kjq}(z)|\}, \end{aligned} \tag{16}$$

where s_k is the number of components that $\theta_{kjq}(z)$ is not equal to zero in each mixture.

By Taylor expansion to the first part of the right-hand side of equation (16),

$$\begin{aligned} &h\sum_{n=1}^{N} \left(\ell(\boldsymbol{\omega}(z) + \alpha\mathbf{u}, \mathbf{x}_n) - \ell(\boldsymbol{\omega}(z), \mathbf{x}_n)\right) K_h(z_n - z) \\ =& \alpha h \sum_{n=1}^{N} q_1(\boldsymbol{\omega}(z), \mathbf{x}_n) \mathbf{u} K_h(z_n - z) + \frac{1}{2}\alpha^2 h \sum_{n=1}^{N} \left(\mathbf{u}^T q_2(\boldsymbol{\omega}(z), \mathbf{x}_n) \mathbf{u}\right) K_h(z_n - z) \\ &+ \frac{1}{6}\alpha^3 h \sum_{n=1}^{N} \left(\sum_{i,j,l} \frac{\partial^3 \ell(\boldsymbol{\omega}(z) + \tilde{\boldsymbol{\xi}}_n, \mathbf{x}_n)}{\partial\omega_i \partial\omega_j \partial\omega_l} u_i u_j u_l\right) K_h(z_n - z) \\ =& \left[\sqrt{(h/N)} \sum_{n=1}^{N} q_1(\boldsymbol{\omega}(z), \mathbf{x}_n) K_h(z_n - z)\right] \mathbf{u} + \frac{1}{2}\mathbf{u}^T \left[N^{-1} \sum_{n=1}^{N} q_2(\boldsymbol{\omega}(z), \mathbf{x}_n) K_h(z_n - z)\right] \mathbf{u} \\ &+ \frac{h\alpha^3}{6} \sum_{n=1}^{N} \left[\sum_{i,j,l} \frac{\partial^3 \ell(\boldsymbol{\omega}(z) + \tilde{\boldsymbol{\xi}}_n, \mathbf{x}_n)}{\partial\omega_i \partial\omega_j \partial\omega_l} K_h(z_n - z) u_i u_j u_l\right] \end{aligned}$$

where $\tilde{\boldsymbol{\xi}}_n = t_n \alpha \mathbf{u}$ for some $t_n \in (0, 1)$ and

$$\Delta_N = \sqrt{(h/N)} \sum_{n=1}^{N} q_1(\boldsymbol{\omega}(z), \mathbf{x}_n) K_h(z_n - z),$$

$$\Gamma_N = N^{-1} \sum_{n=1}^{N} q_2(\boldsymbol{\omega}(z), \mathbf{x}_n) K_h(z_n - z),$$

$$R(\boldsymbol{\omega}(z), \tilde{\boldsymbol{\xi}}_n) = \sum_{i,j,l} \frac{\partial^3 \ell(\boldsymbol{\omega}(z) + \tilde{\boldsymbol{\xi}}_n, \mathbf{x}_n)}{\partial \omega_i \partial \omega_j \partial \omega_l} K_h(z_n - z) u_i u_j u_l.$$

Denote by $\Gamma_N(i,j)$ the (i,j)th element of Γ_N. By condition D. and using change-variable technique it can be shown that

$$\begin{aligned}\mathrm{E}\Gamma_N(i,j) =& \int_{X_p} \cdots \int_{X_1} \int_{\mathcal{Z}} \frac{\partial^2 \ell(\boldsymbol{\omega}(z), \mathbf{x})}{\partial \omega_i \omega_j} \eta(\mathbf{x} \mid \boldsymbol{\omega}(u)) f(u) K_h(u - z)\, du\, dx_1 \cdots dx_p \\ =& f(z) \int_{X_p} \cdots \int_{X_1} \frac{\partial^2 \ell(\boldsymbol{\omega}(z), \mathbf{x})}{\partial \omega_i \omega_j} \eta(\mathbf{x} \mid \boldsymbol{\omega}(z)) \left[\int K(t)\, dt \right] dx_1 \cdots dx_p + o(1)\end{aligned}$$

as $h \to 0$.

Hence, $\mathrm{E}\Gamma_N = -f(z)I(z) + o(1)$. By condition A. and D. and using change-variable technique it can be shown that

$$\begin{aligned}&\mathrm{var}(\Gamma_N(i,j)) \\ \leq& \frac{1}{N^2} \sum_{n=1}^{N} \mathrm{E}(q_2^2(\boldsymbol{\omega}(z), \mathbf{X}_n) K_h^2(Z_n - z)) \\ =& \frac{1}{N} \int_{X_p} \cdots \int_{X_1} \int_{\mathcal{Z}} \left\{ \frac{\partial^2 \ell(\boldsymbol{\omega}(z), \mathbf{x})}{\partial \omega_i \omega_j} \right\}^2 \eta(\mathbf{x} \mid \boldsymbol{\omega}(u)) f(u) K_h^2(u - z)\, du\, dx_1 \cdots dx_p \\ =& \frac{1}{Nh} \int_{X_p} \cdots \int_{X_1} \left\{ \frac{\partial^2 \ell(\boldsymbol{\omega}(z), \mathbf{x})}{\partial \omega_i \omega_j} \right\}^2 \eta(\mathbf{x} \mid \boldsymbol{\omega}(ht + z)) f(ht + z) \left[\int K^2(t)\, dt \right] dx_1 \cdots dx_p \\ =& \frac{1}{Nh} f(z) \int K^2(t)\, dt \int_{X_p} \cdots \int_{X_1} \left\{ \frac{\partial^2 \ell(\boldsymbol{\omega}(z), \mathbf{x})}{\partial \omega_i \omega_j} \right\}^2 \eta(\mathbf{x} \mid \boldsymbol{\omega}(z))\, dx_1 \cdots dx_p + o(1)\end{aligned}$$

as $h \to 0$, which has the order $O((Nh)^{-1})$.

Therefore, we have

$$\Gamma_N = -f(z)I(z) + o_p(1).$$

By condition E., the expectation of the absolute value of the last term is bounded by

$$O\left(\alpha \mathrm{E} \left[\max_{i,j,l} \left| \frac{\partial^3 \ell(\boldsymbol{\omega}(z) + \tilde{\boldsymbol{\xi}}, \mathbf{X})}{\partial \omega_i \partial \omega_j \partial \omega_l} K_h(Z_n - z) \right| \right] \right) = O(\alpha).$$

Hence, the last term is of order $O_p((Nh)^{-1/2})$. Finally, we have

$$D(\mathbf{u}) \leq \Delta_N \mathbf{u} - \frac{1}{2} f(z) \mathbf{u}^T I(z) \mathbf{u}(1 + o_p(1)) - Nh\lambda \sum_{k=1}^{K} \sum_{j \neq q}^{s_k} \alpha \mathrm{sgn}(\theta_{kjq}(z)) u(1 + o(1)). \tag{17}$$

Here, we have

$$\begin{aligned} \mathrm{E}(\Delta_N) =& \sqrt{(Nh)} \int_{X_p} \cdots \int_{X_1} \int_{\mathcal{Z}} q_1(\boldsymbol{\omega}(z), \mathbf{x}) \eta(\mathbf{x} \mid \boldsymbol{\omega}(u)) f(u) K_h(u - z)\, du\, dx_1 \cdots dx_p \\ =& \sqrt{(Nh)} \int_{\mathcal{Z}} \Lambda(u \mid z) f(u) K_h(u - z)\, du. \end{aligned}$$

Under conditions B., E. and F., $\Lambda(u \mid z)$ has a continuous second derivative. Hence, using the fact that $\Lambda(z|z) = 0$ by Lemma 1 and standard arguments in kernel, it follows that

$$\begin{aligned} \mathrm{E}(\Delta_N) =& \sqrt{(Nh)} f(z) \left\{ \frac{f'(z) \Lambda'_u(z \mid z)}{f(z)} + \frac{1}{2} \Lambda''_u(z \mid z) \right\} \mathcal{K}_2 h^2 (1 + o(1)) \\ =& O(1), \end{aligned}$$

under conditions D. and G., where $\mathcal{K}_2 = \int u^2 K(u)\, du$.

Therefore, $\Delta_N = O_p(1)$. Hence, by choosing a sufficiently large C first term on the right-hand side of (17) is dominated by the second term, which is negative.

Note that third term in the (17) is bounded by

$$\sqrt{(s_1 + \cdots + s_K)} Nh\lambda\alpha \|\mathbf{u}\|,$$

which is of order $O(1)$. It is also dominated by the second term. Hence, by choosing a sufficiently large C,

$$P\left(\sup_{\|\mathbf{u}\| = C} \mathcal{L}(\boldsymbol{\omega}(z) + \alpha \mathbf{u}) < \mathcal{L}(\boldsymbol{\omega}(z)) \right) \geq 1 - \varepsilon$$

holds. This completes the proof of Theorem 3. □

References

Ahmed, A. & Xing, E. P. (2009), ‘Recovering time-varying networks of dependencies in social and biological studies’, *Proceedings of the National Academy of Sciences* **106**(29), 11878–11883.

Arnold, L. E. (1996), ‘Sex differences in adhd: conference summary’, *Journal of Abnormal Child Psychology* **24**(5), 555–569.

Balakrishnan, S., Wainwright, M. J. & Yu, B. (2014), ‘Statistical guarantees for the em algorithm: From population to sample-based analysis’, *arXiv preprint arXiv* **1408**(2156).

Bauermeister, J. J., Shrout, P. E., Chávez, L., RubioStipec, M., Ramírez, R., Padilla, L., Anderson, A., García, P. & Canino, G. (2007), 'Adhd and gender: are risks and sequela of adhd the same for boys and girls?', *Journal of Child Psychology and Psychiatry* **48**(8).

Biswal, B. B., Mennes, M., Zuo, X.-N., Gohel, S., Kelly, C., Smith, S. M., Beckmann, C. F., Adelstein, J. S., Buckner, R. L., Colcombe, S. et al. (2010), 'Toward discovery science of human brain function', *Proceedings of the National Academy of Sciences* **107**(10), 4734–4739.

Brillinger, D. R. (1977), 'Discussion of stone (1977)', *The Annals of Statistics* **5**(4), 622–623.

Cai, T., Liu, W. & Luo, X. (2011), 'A constrained ℓ_1 minimization approach to sparse precision matrix estimation', *Journal of the American Statistical Association* **106**(494), 594–607.

Chandrasekaran, V., Parrilo, P. A. & Willsky, A. S. (2012), 'Latent variable graphical model selection via convex optimization (with discussion)', *The Annals of Statistics* **40**(4), 1935–1967.

Consortium, I. H. . (2010), 'Integrating common and rare genetic variation in diverse human populations', *Nature* **467**(7311), 52–58.

Danaher, P., Wang, P. & Witten, D. M. (2014), 'The joint graphical lasso for inverse covariance estimation across multiple classes', *Journal of the Royal Statistical Society: Series B* **76**(2), 373–397.

Dempster, A. (1972), 'Covariance selection', *Biometrics* **28**, 157–175.

Dobra, A., Hans, C., Jones, B., Nevins, J. R., Yao, G. & West, M. (2004), 'Sparse graphical models for exploring gene expression data', *Journal of Multivariate Analysis* **90**(1), 196–212.

Fan, J., Feng, Y. & Wu, Y. (2009), 'Network exploration via the adaptive lasso and scad penalties', *The Annals of Applied Statistics* **3**(2), 521–541.

Fan, J., Xue, L. & Zou, H. (2014), 'Strong oracle optimality of folded concave penalized estimation', *The Annals of Statistics* **42**(3), 819–849.

Fan, J., Zhang, C. & Zhang, J. (2001), 'Generalized likelihood ratio statistics and wilks phenomenon', *The Annals of Statistics* **29**, 153–193.

Fraley, C. & Raftery, A. E. (2002), 'Model-based clustering, discriminant analysis, and density estimation', *Journal of the American Statistical Association* **97**(458), 611–631.

Frazier, T. W., Demaree, H. A. & Youngstrom, E. A. (2004), 'Meta-analysis of intellectual and neuropsychological test performance in attention-deficit/hyperactivity disorder', *Neuropsychology* **18**(3), 543.

Friedman, J., Hastie, T. & Tibshirani, R. (2008), 'Sparse inverse covariance estimation with the graphical lasso', *Biostatistics* **9**(3), 432–441.

García-Sánchez, C., Estévez-González, A., Suárez-Romero, E. & Junqué, C. (1997), 'Right hemisphere dysfunction in subjects with attention-deficit disorder with and without hyperactivity', *Journal of Child Neurology* **12**(2), 107–115.

Goldfarb, D., Ma, S. & Scheinberg, K. (2013), 'Fast alternating linearization methods for minimizing the sum of two convex functions', *Mathematical Programming* **141**(1-2), 349–382.

Huang, M., Li, R. & Wang, S. (2013), 'Nonparametric mixture of regression models', *Journal of the American Statistical Association* pp. 929–941.

Kolar, M., Song, L., Ahmed, A. & Xing, E. P. (2010), 'Estimating time-varying networks', *The Annals of Applied Statistics* **4**(1), 94–123.

Lindsay, B. G. (1995), *Mixture Models: Theory, Geometry and Applications*, NSF-CBMS regional conference series in probability and statistics.

Liu, H., Han, F., Yuan, M., Lafferty, J. & Wasserman, L. (2012), 'High-dimensional semiparametric gaussian copula graphical models', *The Annals of Statistics* **40**(4), 2293–2326.

Loader, C. R. (1996), 'Local likelihood density estimation', *The Annals of Statistics* **24**(4), 1602–1618.

Loader, C. R. (2006), *Local Regression and Likelihood*, Springer.

Ma, S., Xue, L. & Zou, H. (2013), 'Alternating direction methods for latent variable gaussian graphical model selection', *Neural Computation* **25**(8), 2172–2198.

Mack, Y. P. & Silverman, B. W. (1982), 'Weak and strong uniform consistency of kernel regression estimates', *Zeitschrift für Wahrscheinlichkeitstheorie und verwandte Gebiete* **61**(3), 405–415.

Mallapragada, P. K., Jin, R. & Jain, A. (2010), Non-parametric mixture models for clustering, *in* 'Proceedings of the 2010 Joint IAPR International Conference on Structural, Syntactic, and Statistical Pattern Recognition', Springer-Verlag, pp. 334–343.

McLachlan, G. & Peel, D. (2004), *Finite Mixture Models*, John Wiley & Sons.

Meinshausen, N. & Bühlmann, P. (2006), 'High-dimensional graphs and variable selection with the lasso', *The Annals of Statistics* **34**(3), 1436–1462.

Ng, B., Varoquaux, G., Poline, J. B. & Thirion, B. (2013), 'A novel sparse group gaussian graphical model for functional connectivity estimation', *In Information Processing in Medical Imaging* pp. 256–267.

Peng, J., Wang, P., Zhou, N. & Zhu, J. (2009), 'Partial correlation estimation by joint sparse regression models.', *Journal of the American Statistical Association* **104**(486), 735–746.

Polanczyk, G., de Lima, M. S., Horta, B. L., Biederman, J. & Rohde, L. A. (2007), 'The worldwide prevalence of adhd: a systematic review and metaregression analysis', *The American Journal of Psychiatry* **164**(6), 942–948.

Rodríguez, A., Lenkoski, A., Dobra, A. et al. (2011), 'Sparse covariance estimation in heterogeneous samples', *Electronic Journal of Statistics* **5**, 981–1014.

Ruan, L., Yuan, M. & Zou, H. (2011), 'Regularized parameter estimation in high-dimensional gaussian mixture models', *Neural Computation* **23**(6), 1605–1622.

Ryali, S., Chen, T., Supekar, K. & Menon, V. (2012), 'Estimation of functional connectivity in fmri data using stability selection-based sparse partial correlation with elastic net penalty', *Neuroimage* **59**(4), 3852–3861.

Sauver, J. L. S., Barbaresi, W. J., Katusic, S. K., Colligan, R. C., Weaver, A. L. & Jacobsen, S. J. (2004), 'Early life risk factors for attention-deficit/hyperactivity disorder: a population-based cohort study', *Mayo Clinic Proceedings* **79**(9), 1124–1131.

Schäfer, J. & Strimmer, K. (2005), 'An empirical bayes approach to inferring large-scale gene association networks', *Bioinformatics* **21**(6), 754–764.

Städler, N., Bühlmann, P. & Van De Geer, S. (2010), 'ℓ_1-penalization for mixture regression models (with discussion)', *Test* **19**(2), 209–256.

Tibshirani, R. & Hastie, T. (1987), 'Local likelihood estimation', *Journal of the American Statistical Association* **82**(398), 559–567.

Tseng, P. (2001), 'Convergence of a block coordinate descent method for nondifferentiable minimization', *Journal of Optimization Theory and Applications* **109**(3), 475–494.

Varoquaux, G., Gramfort, A., Poline, J. B. & Thirion, B. (2010), 'Brain covariance selection: better individual functional connectivity models using population prior', *In Advances in Neural Information Processing Systems* pp. 2334–2342.

Voorman, A., Shojaie, A. & Witten, D. (2014), 'Graph estimation with joint additive models', *Biometrika* **101**(1), 85–101.

Wang, P., Chao, D. L. & Hsu, L. (2011), 'Learning oncogenic pathways from binary genomic instability data', *Biometrics* **67**(1), 164–173.

Witten, D. M., Friedman, J. H. & Simon, N. (2011), 'New insights and faster computations for the graphical lasso', *Journal of Computational and Graphical Statistics* **20**(4), 892–900.

Wu, C. J. (1983), 'On the convergence properties of the em algorithm', *The Annals of Statistics* **95**(103).

Xue, L. & Zou, H. (2012), 'Regularized rank-based estimation of high-dimensional nonparanormal graphical models', *The Annals of Statistics* **40**(5), 2541–2571.

Xue, L., Zou, H. & Cai, T. (2012), 'Nonconcave penalized composite conditional likelihood estimation of sparse ising models', *The Annals of Statistics* **40**(3), 1403–1429.

Yuan, M. & Lin, Y. (2007), 'Model selection and estimation in the gaussian graphical model', *Biometrika* **94**(1), 19–35.

Zhou, S., Lafferty, J. & Wasserman, L. (2010), 'Time varying undirected graphs', *Machine Learning* **80**(2), 295–319.